

# **Effect on Pavement Wear of an Increase in Mass Limits for Heavy Vehicles**

Transfund New Zealand Research Report No. 207



# **Effect on Pavement Wear of an Increase in Mass Limits for Heavy Vehicles**

J. de Pont, TERNZ Ltd  
B. Steven, University of Canterbury  
D. Alabaster & A. Fussell, Transit New Zealand

ISBN 0-478-25065-7

ISSN 1174-0574

© 2001, Transfund New Zealand  
PO Box 2331, Lambton Quay, Wellington, New Zealand  
Telephone 64-4-473 0220; Facsimile 64-4-499 0733

de Pont, J., Steven, B., Alabaster, D., Fussell, A. 2001. Effect on pavement wear of an increase in mass limits for heavy vehicles. *Transfund New Zealand Research Report No. 207*. 55pp.

**Keywords:** accelerated pavement testing, CAPTIF, loading, New Zealand, pavement, pavement performance, roads, road user charges, thin-surfaced pavements, traffic, vehicles

## **An Important Note for the Reader**

The research detailed in this report was commissioned by Transfund New Zealand.

Transfund New Zealand is a Crown entity established under the Transit New Zealand Act 1989. Its principal objective is to allocate resources to achieve a safe and efficient roading system. Each year, Transfund New Zealand invests a portion of its funds on research that contributes to this objective.

While this report is believed to be correct at the time of its preparation, Transfund New Zealand, and its employees and agents involved in its preparation and publication, cannot accept any liability for its contents or for any consequences arising from its use. People using the contents of the document, whether direct or indirect, should apply and rely on their own skill and judgement. They should not rely on its contents in isolation from other sources of advice and information. If necessary, they should seek appropriate legal or other expert advice in relation to their own circumstances, and to the use of this report.

The material contained in this report is the output of research and should not be construed in any way as policy adopted by Transfund New Zealand but may form the basis of future policy.



## CONTENTS

<b>Executive Summary</b> .....	7
<b>Abstract</b> .....	10
<b>1. Introduction</b> .....	11
1.1 Background .....	11
1.2 The Canterbury Accelerated Pavement Testing Indoor Facility (CAPTIF).....	13
<b>2. Objectives</b> .....	15
<b>3. Method</b> .....	16
3.1 Pavement Design .....	16
3.2 Pavement Construction .....	17
3.2.1 Preparation .....	17
3.2.2 Subgrade Construction .....	18
3.2.3 Basecourse Construction .....	19
3.2.4 Sealing .....	20
3.3 In-Pavement Instrumentation .....	20
3.4 Zero Measurements .....	21
3.4.1 Pavement Structural Condition .....	21
3.4.2 Pavement Functional Condition .....	21
3.4.3 Vehicle Loading Configuration .....	21
3.5 Pavement Testing .....	22
3.6 Post-mortem .....	23
<b>4. Results and Analysis</b> .....	25
4.1 Materials Characterisation .....	25
4.2 Pavement Variability .....	27
4.3 Zero Measurements .....	29
4.4 Test Measurements .....	29
4.4.1 Dynamic Wheel Forces .....	29
4.4.2 CAPTIF Deflectometer and FWD Measurements .....	31
4.4.3 Longitudinal Profiles and Roughness .....	33
4.4.4 Vertical Surface Deformations and Rutting .....	33
4.4.5 Fitting a Power Law .....	34
4.5 Post-mortem Measurements .....	40
4.6 Discussion .....	43
<b>5. Conclusions</b> .....	45
<b>6. Recommendations</b> .....	47
<b>7. References</b> .....	49
<b>Appendix A Graphs of Post-mortem Trenches</b> .....	51





## Executive Summary

### Introduction

The road transport industry in New Zealand has been lobbying for increases in the allowable mass limits for heavy vehicles on the basis of increased efficiency and benefits to the economy. Some of the proposals for increased mass limits involve increased axle load limits, which would clearly lead to additional pavement wear. Road controlling authorities, while sharing the industry's aims for increased efficiencies in the road transport system, are concerned that any additional pavement wear generated by higher axle loads is paid for, so that the standard of the network can be maintained.

Under the current road user charges (RUC) regime, the users would be charged for the additional wear on the basis of the fourth power law, which states that the amount of damage caused by the passage of an axle is proportional to the fourth power of its weight. Thus an axle load increase of 10% would lead to an increase in road user charges for that axle of 46%. This fourth power law has its origins in the AASHO<sup>1</sup> road test which was conducted in the United States in the late 1950s using roads and vehicles which bear little resemblance to those in use in New Zealand today.

### Accelerated Pavement Test

In this study, carried out between 1999-2001, an accelerated pavement test was undertaken at the Canterbury Accelerated Pavement Testing Indoor Facility (CAPTIF) to compare the effect of mass on pavement wear for four different sections of pavement which are more typical of those found in New Zealand. The two "vehicles" at CAPTIF, which are known as SLAVES (Simulated Loading and Vehicle Emulators), were configured with identical suspensions but with different axle loads. One was loaded to 40kN to simulate the current 80kN axle load limit, while the other was loaded to 50kN to simulate a possible increase to a 100kN axle load limit. The test was conducted with the two SLAVES trafficking parallel independent wheel paths so that the relative wear generated by the two could be compared.

### Construction of Pavement

A pavement was constructed at CAPTIF in four segments, each of similar design but using different basecourse materials. The expected design life under 50kN loading of the segment made with standard M/4 crushed rock, as constructed, was 1,000,000 load cycles with the other three pavement segments being expected to be similar. The pavement was extensively monitored during construction. After construction 5,000 load cycles were applied across the whole width of the track that was to be trafficked, and then a set of zero measurements was undertaken to characterise the whole system.

### Test of Pavement

After this the test proper commenced. Testing consists of applying a number of loading cycles, then stopping the loading to collect a set of measurements and then repeating the cycle. At the start of the test the number of load cycles between measurement sets is relatively small (10,000 cycles) but, as the test progresses and the rate of change of the pavement stabilises, this is increased until in mid-test 100,000 load cycles are applied between measurements. Testing proceeded until 1,000,000 load cycles had been applied. Although the design guide indicated that the as-constructed pavement should have reached the failure criteria at this point, this was not the case with average rut depths around 10mm compared to a failure criterion of 25mm. As the rate of increase of rutting was steady and slow, it did not appear that the pavement would achieve the failure criterion without applying a very large number of additional cycles and thus the test was terminated.

---

<sup>1</sup> AASHO Association of American State Highway Organisations (before 1973)

## Post-mortem Testing

On completion of the testing for this project, a further 320,000 load cycles were applied in a series of tests required for another Transfund project before a post-mortem was undertaken. The post-mortem involved cutting three trenches in three of the pavement segments, and measuring the rutting in the layers and the changes in pavement materials.

## Analysis

For the analysis, vertical surface deformation (VSD) was used as the main measure of pavement wear. VSD is directly related to rutting and the variability in VSD leads to increased roughness. As VSD in previous CAPTIF tests has been shown to be correlated to dynamic loading and to the variability in pavement structure, increased VSD results directly in increased roughness. Both roughness and rutting are key measures used by road controlling authorities to determine the need for pavement maintenance. By comparing the rate of progression of VSD under the two loading regimes, the impact of mass increases on pavement wear can be determined and the impact on road maintenance costs can be estimated.

## Conclusions

From the analysis the following conclusions could be drawn:

- Although a conventional power law relationship could be fitted to describe the differences in VSD between the two levels of loading for each of the four pavement segments, there was a large variation (between 2.8 and 9) in the exponent value required to give the best fit. As the pavement design of the four segments was substantially similar in character, it does not seem reasonable that the exponents for a power law model should vary so much. It also makes it impossible to predict the appropriate exponent value in advance. Thus the power law approach does not appear to be an accurate or useful way of modelling the VSD wear of this type of pavement.
- Reviewing the progression of VSD with load cycles shows that the pavement underwent two distinct phases of VSD. An initial period of rapid change was observed, here called compaction, followed by a period with a constant (linear) rate of change, here called wear. Least squares regression can be used to fit a straight line to the linear part of the VSD versus load cycles curve. The intercept of this line with the y-axis then gives the compaction component and the slope gives the wear. For each of the four pavement segments, a power law can be used to relate the compaction and wear between the normally and more heavily loaded wheel paths. Remarkably the best-fit exponent values for compaction and wear were quite similar for each pavement segment, and did not vary too much between segments.
- This compaction-wear model implies that the compaction depends only on the magnitude of the applied load and not on the number of load cycles, while the wear depends on both the load and the number of load applications. A corollary of this is that, if the axle load level is increased at any stage, further compaction will occur to reflect this higher load. As this model was developed well after the completion of the testing programme, this hypothesis was not specifically tested for, but in the project that followed this one at CAPTIF, the same pavement was used and higher loads were applied to the more lightly loaded wheel path. In this follow-up, the VSD did show an apparent increased compaction as would be expected.
- The exponent values for the compaction-wear model were between 1 and 3.4 for compaction and 1.8 and 3 for wear. (The values for pavement segment C were a little lower than this but repairs to the pavement surface during the test meant that very few data points could be used for this segment.) The implication of this is that, if the axle load limit were increased, the underlying wear rate of the compaction-wear model would increase as indicated by a power of between 1.8 and 3.

As the road user charges paid by these vehicles are based on a conventional model with a power of 4, the additional road user charges would more than offset the additional wear. In fact, there is some ground for considering a review of the road user charges schedule. But note that the effect of the compaction phase will also be observed in new construction and rehabilitation so this effect cannot be ignored, and an increase in axle load limit would also cause an immediate (over a year or two) additional compaction. Thus it would appear that the network had suddenly deteriorated substantially. This is a one-off effect but would need to be planned for by the road controlling authorities if pavement condition is to be maintained. If the road controlling authorities are not anticipating this additional compaction effect, the sudden apparent additional deterioration of the network will cause them great concern over the future maintenance demands.

- The existing fourth power approach is based on a chord approach, i.e. the amount of damage is considered only at the initial and terminal conditions. This research has shown that some merit may be gained in looking at a secant (tangential) rate of damage, but this approach would be difficult to incorporate into a charging model.
- Measurements of dynamic wheel force and pavement roughness showed qualitative trends that were as expected. However, as parts of the surface of the outer wheel path in segment C were substantially repaired at 200,000 load cycles and at 700,000 load cycles, any meaningful quantitative results could not be extracted from measurements that were taken for a complete circuit of CAPTIF.
- FWD measurements were taken at four intervals during the test. The results for the four pavement segments were very consistent with each other. In the early stages of the test a relatively rapid increase in peak deflection was observed indicating a reduction in stiffness of the pavement. This rate of increase slows and by the end of the test is negative, indicating that the stiffness of the pavement is increasing slowly. In all four cases, the changeover from decreasing stiffness to increasing stiffness occurs sooner on the inner wheel path, which was trafficked with the lighter load.
- If the current conventional fourth power law approach is retained, then for New Zealand materials the power law should be increased subject to the results obtained in the 2001-2002 follow-up study which will examine the power laws in a wider range of conditions.

## **Recommendations**

From these findings, a number of questions requiring further investigation arise:

- Further validation of the compaction-wear model is required. It is recommended that, in future CAPTIF trials where a wheel path has been trafficked with a constant load, after completion of the test some relatively small number (perhaps 300,000) of load cycles with a higher load are applied. If the compaction-wear model is valid it will be possible to predict and test the amount of compaction that will occur. Work in progress at CAPTIF (2001) has attempted to address this issue but additional validation will be required.
- Although the compaction-wear model provides a good fit to the observed behaviour and is a useful predictor tool, the mechanisms underlying it are not understood. Further research is required to determine how the pavement materials are behaving and what is leading to the compaction and wear components of VSD. Note that the names, “compaction” and “wear” are speculative and not based on any real knowledge of the underlying material behaviour.
- The FWD measurements indicate some rather interesting behaviour with the pavement stiffness increasing in the later stages of the test. This needs further investigation as it implies that after an initial reduction the structural capacity of the pavement increases with additional load cycles.

- More detailed analysis of the cost implications of the compaction-wear model are needed. The underlying wear rate of the compaction-wear model appears to be related to load by a power lower than four. However, the compaction component is also related to load by a power law.
- The VSD associated with compaction is equivalent to the wear associated with a considerable number of load cycles. If this compaction can be induced without causing rutting or roughness, the performance of the pavement would be enhanced considerably.
- The performance of thin asphaltic concrete surfacings under the higher axle loads needs to be investigated further. The pavement surfacing exhibited distress and failures under the 50kN axle load, but not the 40kN axle load.

Overall the most significant finding of this study is the development of the compaction-wear model for VSD. This provides a much better fit to the observed behaviour than the conventional power law model, and has very significant implications for pavement management practice in New Zealand, and wherever thin-surface unbound pavement structures are widely used. The implication of the model is that if an increase in axle load limit occurred, there would be an immediate rapid increase in VSD that would manifest itself as an increase in rutting and roughness due to additional compaction of the pavements.

The long-term effect would be an increase in wear rate proportional to a second or third power of the axle loads. However, the short-term increased compaction would require substantial additional pavement maintenance over the first year or two to maintain the performance of the road network. For example, if the compaction was equivalent to six months wear, then over the first two years after the change, 150% of the current annual budget for roughness and rutting rehabilitation would need to be spent.

Further validation work should be undertaken as well as research to understand the material behaviour mechanisms that produce this behaviour.

## **Abstract**

In order to improve the efficiency of the road transport industry in New Zealand, a range of mass limit increases for heavy vehicles has been proposed. Some of the options for mass increases include increasing the axle load limit, which would inevitably lead to increased road wear. As New Zealand has a mass-distance road user charging regime, where the users pay for the road wear they generate, this is in itself not a problem provided that the charges accurately reflect the wear. At present (2001) road user charges are based on the fourth power law, which was developed from the AASHO road test in the United States in the 1950s. The pavements and vehicles used for that test differ considerably from those in use in New Zealand today.

In this study, carried out between 1999-2001, an accelerated loading test was undertaken at the Canterbury Accelerated Pavement Testing Indoor Facility (CAPTIF) to compare the wear generated by different levels of loading. The pavement consisted of four different segments that were subjected to one million load cycles in two parallel wheel paths. The axle load on one wheel path was 80kN while the load on the other was 100kN. As a result the compaction-wear model for VSD (Vertical Surface Deformation) has been developed, which provides a much better fit to the observed behaviour, than the conventional power law model, for thin-surface unbound pavement structures.

## 1. Introduction

### 1.1 Background

The road transport freight industry in New Zealand understandably wishes to increase its efficiency. One of the ways to do this is through increases in the allowable mass limits for heavy vehicles. This in turn can result in economic benefits to the whole country provided the impact of the changes in mass limits are accurately known and considered in assigning the new limits and in determining appropriate road user charges (RUC). One of the impacts concerning road controlling authorities (RCA) is the effect on increasing mass limits on the life of their pavements or how much more pavement rehabilitation and maintenance will be required.

In response to the industry's requests for larger and heavier vehicles, Transit New Zealand (Transit) undertook, between 1999-2001, a study to assess the economic and safety impacts of increasing mass limits. This study investigated two scenarios:

- Scenario A, where heavier vehicles subject to the same dimensional limits as are currently in place would be permitted to operate across the entire network;
- Scenario B, where longer and heavier vehicles would be permitted to operate only a selected set of key routes.

Within these two scenarios several axle mass limit options as shown in Table 1.1 were considered.

**Table 1.1 Axle mass limit options in Transit Heavy Vehicle Limits project.**

Option	Allowable weights (tonnes)			
	steer axle	single axle	tandem axle	triaxle
Present	6.0	8.2	15	18
1	6.0	8.2	15	19
2	6.0	8.2	15	20
3	6.0	8.8	16	20

Transit's evaluation of these proposed changes in mass limits included research into the safety, geometric, economic, pavement and bridge impacts. In determining the pavement wear impact of these mass limits changes, existing theories for the relationship between vehicle loads and pavement wear were utilised. The most widely used existing theory for determining the effect of mass limit increases on pavement life is the fourth power rule. This is used to determine the pavement loading as a number of Equivalent Standard Axles (ESAs). The formula for converting an actual axle load to ESA is:

$$ESA = \left[ \frac{\text{Actual axle load}}{\text{Reference axle load}} \right]^4$$

This fourth power relationship between axle loads and pavement life has never been validated on New Zealand's thin-surfaced unbound granular pavements. Power values between 1 and 8 have been suggested by different researchers throughout the world for different pavement structures and failure mechanisms (Cebon 1999, Kinder & Lay 1988, Pidwerbesky 1996). Even the AUSTRROADS Pavement Design Guide (1992), which is the basis of New Zealand design practice, uses a power of 4 for unbound basecourse performance and a power of 7.14 for subgrade performance.

The use of a fourth power relationship predicts that the 7.3% increase in allowable loading for a single axle, as per option 3 (Table 1.1), will result in a 33% increase in pavement wear, and consequently a road controlling authority can expect a 33% increase in the length of pavement rehabilitation required per year. The actual situation is not as extreme as this because, in the first place, not all vehicles will change to the higher limits, and second the higher axle load limits will result in higher payloads and consequently fewer trips for the same freight volume. Nevertheless, this change will represent a significant increase in annual expenditure on roads for a road controlling authority and requires budgeting for. The uncertainty in the validity of the fourth power rule poses difficulties when requesting increases in funding for the next financial year. Justifying an increase in the road user charges based on a fourth power rule that has not been validated in New Zealand is expected to be increasingly difficult, particularly as research results from accelerated pavement tests are suggesting different relationships.

This study investigates, via accelerated pavement testing on typical New Zealand pavement designs, the relative effect on pavement life of an increase in axle load from 8.2 tonnes (the present load limit) to 10 tonnes. This increase is somewhat higher than the proposed limit in option 3. There are two reasons for using this higher axle load. The first is that, in response to the heavy vehicle limits study, the bus and coach industry has suggested that this level of increase should be considered. The second is that the larger mass difference between the two wheel paths was more likely to ensure that the difference in wear is sufficiently large to be able to draw clear conclusions. By interpolating the results of this research, the effect on pavement life of loading increases could be assessed directly.

A key issue for this study is what constitutes pavement wear. The OECD DIVINE project (OECD 1998) differentiates between functional and structural condition for pavements. Functional condition reflects the ability of the pavement to provide service to the road user and covers factors such as roughness, rutting and skid resistance. Structural condition relates to the ability of the pavement to support the loads applied to it and relates to cracking and other forms of distress. In some instances, a loss of functional condition may also indicate a loss of structural condition. In New Zealand, pavement maintenance and rehabilitation is driven primarily by measures of functional condition and thus, in this study, wear is taken to mean a reduction in functional condition.

1. Introduction

1.2 The Canterbury Accelerated Pavement Testing Indoor Facility (CAPTIF)

CAPTIF is located in Christchurch. It consists of a 58m long (on the centreline) circular track contained within a 1.5m deep x 4m wide concrete tank, so that the moisture content of the pavement materials can be controlled and the boundary conditions are known. A centre platform carries the machinery and electronics needed to drive the system. Mounted on this platform is a sliding frame that can move horizontally by 1m. This radial movement enables the wheel paths to be varied laterally and can be used to have the two “vehicles” operating in independent wheel paths. An elevation view is shown in Figure 1.1.

At the ends of this frame, two radial arms connect to the Simulated Loading and Vehicle Emulator (SLAVE) units shown in Figure 1.2. These arms are hinged in the vertical plane so that the SLAVES can be removed from the track during pavement construction, profile measurement, etc., and in the horizontal plane to allow vehicle bounce.

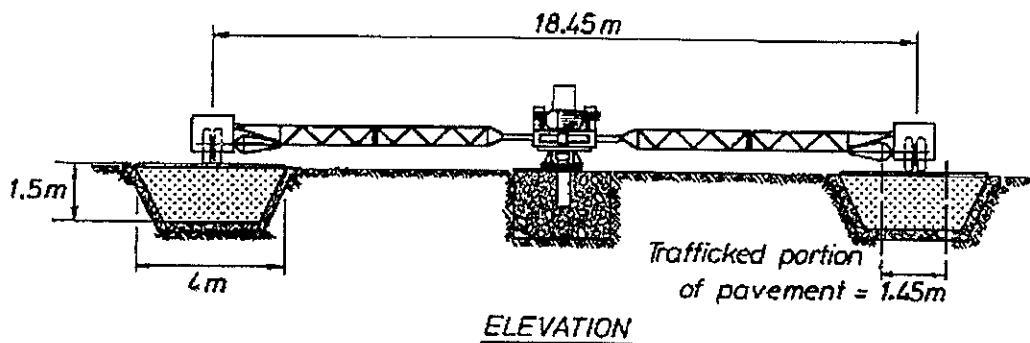


Figure 1.1 Elevation view of CAPTIF.

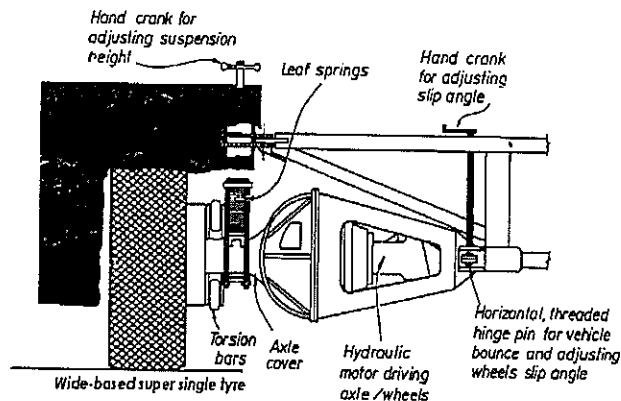


Figure 1.2 The CAPTIF SLAVE unit.

CAPTIF is unique among accelerated pavement test facilities in that it was specifically designed to generate realistic dynamic wheel forces. All other accelerated pavement testing facility designs, that we are aware of, attempt to minimise dynamic loading. The SLAVE units at CAPTIF are designed to have sprung and unsprung mass values of similar magnitude to those on actual vehicles and use, as far as possible, standard heavy vehicle suspension components. The net result of this is that the SLAVES apply dynamic wheel loads to the test pavement that are similar in character and magnitude to those applied by real vehicles. This was a significant factor in its selection for this project. A summary of the characteristics of the SLAVE units is given in Table 1.2. The configuration of each vehicle, with respect to suspensions, wheel loads, tyre types and tyre numbers, can be identical or different for simultaneous testing of different load characteristics.

Pavement instrumentation which is used at CAPTIF includes: Emu coil transducers for measuring vertical compressive strains in the lower layers of the pavement, h-bar strain gauges for measuring horizontal strains at the bottom of the asphalt layer, and partial depth gauges for measuring the pavement layer deflections. As well temperature probes are used to monitor both the pavement and air temperatures. The vehicle instrumentation consists of accelerometers mounted on both the sprung and unsprung masses of each "vehicle" and displacement transducers to measure suspension displacements. As the "vehicles" are a fairly simple quarter vehicle structure, dynamic wheel forces can be calculated by combining the two accelerometer signals weighted by appropriate mass factors.

Other measurement systems used at CAPTIF during testing are: a Falling Weight Deflectometer (FWD), a Loadman falling weight deflectometer, the CAPTIF Deflectometer which is a modified Benkelman beam, a transverse profilometer, a DIPStick profiler, and a laser profilometer. The laser profilometer was acquired about six years ago and has now effectively replaced the DIPStick for longitudinal profile measurements. For convenience of measurement the track is divided into 58 equally spaced stations which are 1m apart on the centreline wheel path.

A more detailed description of the CAPTIF and its systems is given by Pidwerbesky (1995).

**Table 1.2 Characteristics of SLAVE units.**

Test Wheels	Dual- or single-tyres; standard or wide-base; bias or radial ply; tube or tubeless; maximum overall tyre diameter of 1.06m
Mass of Each Vehicle	21kN to 60kN, in 2.75kN increments
Suspension	Air bag; multi-leaf steel spring; single or double parabolic
Power drive to wheel	Controlled variable hydraulic power to axle; bi-directional
Transverse movement of wheels	1.0m centre-to-centre; programmable for any distribution of wheel paths
Speed	0-50km/h, programmable, accurate to 1km/h
Radius of Travel	9.2m



## 2. Objectives

The principal objective of the study is to determine the effect on pavement life and pavement performance of increasing the maximum allowable axle load for different pavement strengths (or aggregate depth), using data from an accelerated pavement test.

Based on this effect the aim is then to predict the increase in road expenditure resulting from an increase in the allowable axle loads and thus justify to the Transport Industry the increase in Road User Charges (RUCs) that would be required to offset this expenditure.

RUCs are currently based on a fourth power law, so an increase in axle load will lead to a substantial increase in RUCs for vehicles with these more heavily loaded axles.

The purpose of the second objective is to assess whether this increase is at the appropriate level.

### **3. Method**

#### **3.1 Pavement Design**

The objective of the pavement design was to produce the relatively low levels of rutting observed in typical New Zealand pavements while maintaining a balance between the life of the heavily loaded (10 tonne) outer wheel path and the lightly loaded (8.2 tonne) inner wheel path.

The decision to use four sections of different materials was made to accommodate the requirements of another project that also used data from the current test (Arnold et al. 2001). Sections A, B and C were to be instrumented as part of the other project, and would have additional laboratory testing in the form of Repeat Load Triaxial tests on the materials and trenches dug as part of the post-mortem. The original experimental design called for only one pavement material. The four pavement sections were not considered separately in the design because the materials data available at the design stage were not sufficient to consider separate designs for each material. Pavements of the same depth were considered in order to limit the number of variables in the project.

The pavement was designed in an iterative manner using the AUSTROADS Pavement design guide. The iterative designs assumed a 700kPa tyre pressure with a 95.6mm-tyre radius on the inner wheel path and a 850kPa tyre with a 97mm-tyre radius on the outer wheel path. The basecourse layer was, from previous experience, modelled with a modulus of 400MPa using AUSTROADS sub-layering and, as convention dictates, the thin asphaltic layer was not considered in the analysis. The subgrade was modelled with a 10th percentile design in-situ CBR of 10, based on test results at the top of the subgrade layer, and used the standard 10 times CBR relationship to obtain the modulus.

The iterative analysis suggested the inner (8.2 tonne) wheel path would require a basecourse 250mm deep to withstand the design 1,000,000 wheel passes, and a depth of 290mm for the outer wheel path assuming the AUSTROADS subgrade strain criterion. Using the fourth power law to convert the 10 tonne wheel to an equivalent number of standard axles, rather than modelling directly, suggested that the outer wheel path would need to be 270mm deep.

The final design using 275mm basecourse resulted in a pavement that, in the inner wheel path, would theoretically fail at 2.9 million wheel passes and, in the outer wheel path, at 600,000 wheel passes assuming the AUSTROADS subgrade strain criterion and directly modelling the tyres. Using the fourth power law suggested that the outer wheel path would fail at 1.2 million wheel passes.

### 3.2 Pavement Construction

#### 3.2.1 Preparation

The pavement was constructed in three primary segments: Segment A extended from station 00 to station 15; Segment B from 15 to 29; and Segment C from 29 to 43. An additional segment, Segment D, extended through the track access area from 43 to 00. A 4m transition zone was allowed between segments. Within each segment on the track centreline there were 3 primary sites for intensive monitoring and 14 secondary sites for less intensive monitoring. A plan showing the layout of the different sections is shown in Figure 3.1. An elevation showing the cross section of the pavement design, location of the two wheel paths and the in-situ instrumentation is shown in Figure 3.2.

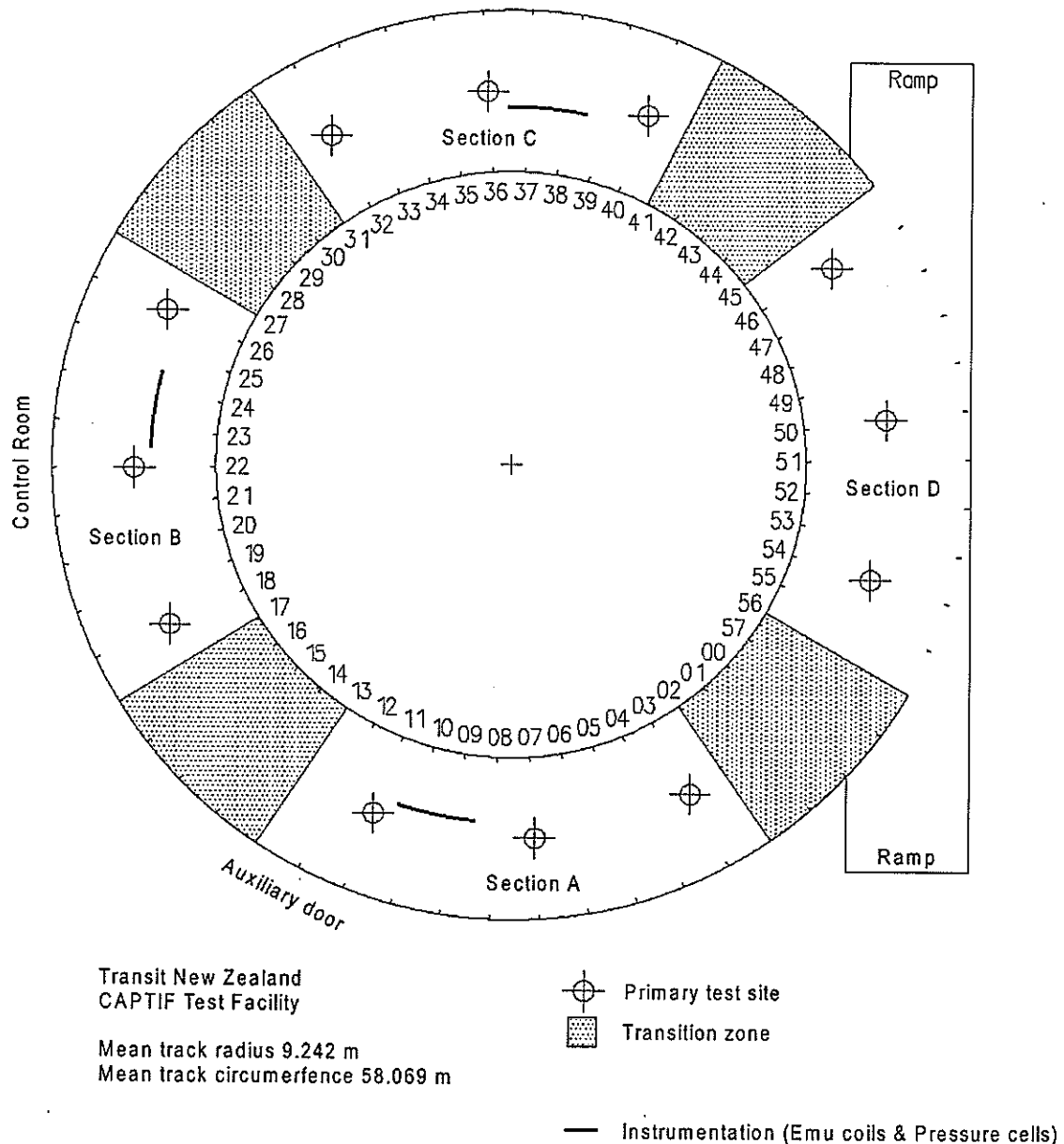


Figure 3.1 Plan showing the layout of the test sections.

The previous pavement was excavated by backhoe digger to a depth of 1m, leaving a 500mm layer of Waikari clay over the concrete base of the pavement tank. The excavated material was stockpiled under cover to maintain the water content.

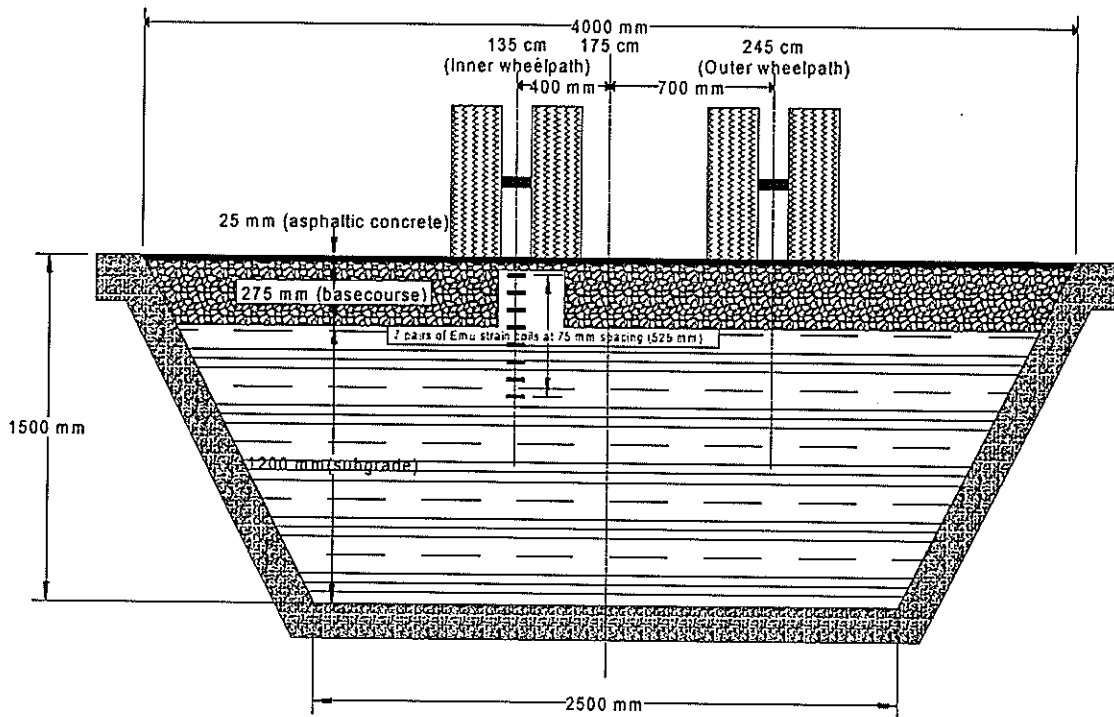


Figure 3.2 Pavement cross section and wheel path locations.

### 3.2.2 Subgrade Construction

The surface of the remaining Waikari clay base was ripped to a depth of 150mm by a backhoe digger equipped with a ripper tooth and then rotary-hoed to a fine tilth. A slightly wetted-up, thin lift of excavated material, was added from the stockpile to bring the finished level up to the first of the planned lift levels. A bulldozer then levelled the surface and it was rolled with two passes of a Rammax trench roller. The number of passes of the compactor is a nominal figure because the Rammax is of skid-steer design and has to be driven back and forth continually to follow the circular track. Nuclear density measurements at the primary sites showed that the dry density averaged  $1760\text{kg/m}^3$  and the water content was 9.6%. This layer was called Lift 1.

The clay for the subgrade was placed in four lifts each of 150mm using the standard CAPTIF procedure:

- a pad was constructed at design level for the bulldozer to sit on;
- material was brought in from the stockpile by a loader travelling over the previously compacted surface;
- the load was dropped on the pad in front of the bulldozer then pushed over the edge;

### 3. *Method*

---

- levels were monitored by laser level and digital staff throughout back-filling with an allowance for compaction.

Lift 5, the final lift of the subgrade was worked with a combination of bulldozer, tractor rake, and hand rakes to get the finished level within the required tolerance. The strain coils were installed at the appropriate levels during the subgrade construction.

In-situ CBR readings, density readings, sand replacement and Scala penetrometer measurements were taken, followed by Loadman deflection measurements at 100 locations (5 locations at 500mm centres at each primary station; on the centreline at every secondary station). The Dynatest pressure cells were placed at the top of the subgrade on the inner wheel path, between the coil stations in each segment. Transverse profiles of the top of subgrade at every station were recorded as well as spot heights measured with the laser level.

#### **3.2.3 Basecourse Construction**

Lift 6, the first lift of the basecourse, was placed in a 150mm deep layer. Four different sections, each with different basecourse materials were constructed: Segment A used a washed AP40 TNZ M/4 aggregate; Segment B used a AP40 TNZ M/4 aggregate with added Waikari clay fines; Segment C used a AP40 TNZ M/4 aggregate with even more added Waikari clay fines; and Segment D used a standard Canterbury crushed alluvial AP40 TNZ M/4 aggregate. All used the same parent material, a crushed alluvial gravel. The strain coils were placed at the required depths.

Five passes with the Wacker plate compactor were applied and the density was measured after each pass. Spot height and Loadman deflection readings were taken. The Loadman results appeared to be very dependent on the surface condition where they were taken.

Following these measurements, the final 125mm basecourse lift, Lift 7, was placed. In Segment D, a 6m section of recycled concrete was used in place of the M/4. Each material handled differently with both the washed M/4 and the recycled concrete being easy to segregate. An initial static pass of a 4 tonne steel/rubber combo roller was applied to the surface and then the strain coils were placed.

Water was applied to the basecourse to bring it up to optimum moisture content (OMC), several passes with the combo roller were applied and the densities were measured. More water was added and three passes with the Wacker plate compactor were applied. At this stage, there were problems compacting the material in Section C due to the high fines content (12% passing 75µm sieve by mass). It was decided to remove this material and replace the entire section with the Australian AP20 material that had been used in a previous project.

While these problems were occurring with Segment C, the basecourse layers in the other segments were compacted normally. A total of 8 passes of the Wacker plate compactor were applied before the density levelled off at approximately 2100kg/m<sup>3</sup>. Although a considerable quantity of water was added to Segment A, the moisture content still only reached about 4.5%. Segment B required a little water and the remainder none at all.

The repaired Segment C was placed and compacted after the other segments. The Australian material was much easier to handle than the TNZ M/4, holding its moisture better and less inclined to segregate.

Basecourse testing included surface profile measurements, nuclear density, sand replacement, and Loadman deflections at the same locations as the subgrade testing. The tests were done after the track had had 10 days to dry out, and after the surface was swept of loose material.

### **3.2.4 Sealing**

The basecourse surface was heavily tack coated, and 25mm depth of 10mm-asphaltic concrete was placed by an asphaltic concrete paving machine over the entire track. The operators had trouble setting the depth of mix at the beginning of Segment A and a subsequent check of the height of the basecourse surface showed that the surface had moved since the levels were last measured. This could be explained by the extra rolling that was done to compact Segment C, exaggerated by the rather loose surface produced by the washed M/4. The sealing crew used a footpath roller behind the paving machine but, once the paving machine had completed the circle and left the building, the entire surface was rolled with a 3.5 tonne combo (rubber tyre and steel drum) roller.

Nuclear density readings, profile measurements and Loadman deflections on the sealed surface were recorded.

## **3.3 In-Pavement Instrumentation**

The soil strain instrumentation was extended to enable measurement of all three pavement segments. The soil strain instrumentation previously used at CAPTIF, developed by the University of Canterbury under license from the Saskatchewan Highways and Transport facility in Canada, was replaced by a system purchased from the University of Nottingham, known as the Emu Strain System. Strain coils were fabricated at CAPTIF using Nottingham guidelines. Relay boards, triggering systems, and software were developed at the University of Canterbury.

Data from three Dynatest pressure cells, mounted vertically and horizontally at the top of subgrade, were also read by the same computer that was operating the strain coils. The pressure cell readings were triggered in the same manner as the strain readings, by an infrared beam.

### **3.4 Zero Measurements**

Basic measurements of the surface profile and structural capacity of the pavement as constructed were undertaken. The SLAVE units were then loaded to 40kN each and 5,000 preliminary conditioning load cycles (10,000 ESA) were applied evenly across the full trafficable width of the pavement. Following these conditioning laps, a set of zero measurements to characterise the system at the start of the test were undertaken. The dynamic wheel-force measurement and longitudinal laser profiling system were checked for spatial accuracy in relation to the fixed referencing system used at the facility. These checks confirmed that the vehicle-based measurement systems were starting data collection at station 00 and that the interval between individual data points was correct.

#### **3.4.1 Pavement Structural Condition**

The Loadman Falling Weight Deflectometer was used to monitor the structural capacity of the pavement layers during construction, as described in Section 3.2. At the top of the subgrade and basecourse layers, measurements were made transversely at a number of stations. On completion of construction, the CAPTIF deflectometer was used to characterise the structural capacity along the centreline of the track at every station.

#### **3.4.2 Pavement Functional Condition**

Transverse profiles were measured at each of the 58 stations using the CAPTIF transverse profilometer. This is referenced back to the tank wall and gives elevation readings at 25mm spacings across the track.

Longitudinal profiles were measured along five centre lines using the laser profilometer. The five centrelines consisted of one in the centre of each wheel path, one midway between the two wheel paths, one inside the inner wheel path, and one outside the outer wheel path.

#### **3.4.3 Vehicle Loading Configuration**

Both vehicles were fitted with dual 11R22.5 tyres and the same steel leaf spring suspension. After the conditioning laps during which both vehicles were loaded to 40kN, a series of dynamic wheel force measurements was undertaken to characterise the loading configuration.

With both vehicles loaded to 40kN, the effect of varying the transverse position of the SLAVE units was measured with ten sets of readings with the offset changing by 0.1m each time.

The effect of speed variations was recorded by taking measurements at 20km/h and 45 km/h. For these measurements the vehicles were loaded to the test condition with 40kN on vehicle A and 50kN on vehicle B.

The effect of variations in load was measured by setting the load on vehicle A to 21kN, 31kN, 40kN, 44kN and 50kN. The load on vehicle B was 50kN throughout these tests.

Finally the 80mm drop test at crawl speed, as specified by the EC (Council of the European Communities 1992) in their regulations for rating a suspension as “equivalent-to-air”, was applied to characterise the suspension behaviour. This test involves running the vehicle over a ramp that culminates in an 80mm drop and measuring the suspension response. For these measurements the vehicles were in the test load configuration, with vehicle A at 40kN and vehicle B at 50kN.

The vehicles were weighed by standard New Zealand Police portable weigh scales at their operating configuration. The static weight for vehicle A was 4080kg (40.02kN), and the static weight for vehicle B was 5060kg (49.64kN).

### **3.5 Pavement Testing**

For this project the SLAVE units were run in concentric offset wheel paths. Previous projects had used wide-base single tyres when the SLAVE units were run in offset wheel paths. However this project specified the use of standard dual tyre assemblies. As the dual tyre assembly is considerably wider than a wide base single tyre (560mm v 300mm), this meant that there would not be sufficient separation between the two vehicles, even with a narrow wander pattern. To overcome this limitation, a 300mm-long extension section was fitted to arm B. Thus the radial distance between the centrelines of the vehicles was 1100mm and the clear separation between the vehicles was 450mm, with the vehicles operating on a  $\pm 50$ mm normally distributed wander pattern.

The vehicles were run continuously at a mean speed of 45km/h with breaks for testing intervals at 20,000, 30,000, 50,000, 100,000, 150,000, 200,000, 250,000, 300,000, 400,000, ... 1,000,000 cycles. Starting at 20,000 cycles, every third test comprised a full set of tests that included: 58 transverse profiles; 5 longitudinal profiles; pavement strain and pressure readings at 45km/h and 15km/h; and dynamic wheel loads at 45km/h.

At the other test intervals a reduced data set was taken. The reduced data set included 58 transverse profiles; longitudinal profiles in the wheel paths only; and strains and pressures at 45km/h only. The Falling Weight Deflectometer measured all stations in both wheel paths at 25,000, 200,000, 600,000, and 1,000,000 cycles. It was not possible to use the CAPTIF Deflectometer during the testing programme because it operates from Vehicle A and the arm extension prevented the vehicles from switching wheel paths. The implication of this was that the deflection measurements could not be undertaken in the outer wheel path.



### 3. *Method*

---

At the completion of 5000 cycles the surfacing at the beginning of Segment A began to ravel. Analysis of the manual profiles of the basecourse and asphalt layers in this section showed that the asphalt thickness was quite variable and very thin in places. This was due to the difficulty in setting the correct screed level on the paver mentioned earlier. The section of the asphalt from station 01 to 04 was removed over the full trafficked width. The basecourse was re-finished to the required level and new asphalt surfacing was placed by barrow and flat rake. The repair remained stable for the rest of the project.

After 200,000 laps the asphaltic concrete surfacing in Segment C began to show signs of shear failures in the outer (50kN) wheel path only. When the seal was removed, the top of the basecourse looked glazed and dirty with no significant bonding of the asphalt mix to the basecourse material. The damaged sections of seal were replaced, but the problem recurred at 700,000 and 1,000,000 cycles in different places in the outer wheel path in section C.

The tyres exhibited a strange wear pattern during the testing phase of the project. The tread blocks on the inner and outer edges of each tyre wore badly on the trailing edge and some tread blocks were torn from the tyre. This pattern of wear was attributed to the set up of the vehicles. This resulted in the outer tyres of each vehicle being replaced after 700,000 cycles, and the inner tyres being replaced after 860,000 cycles. After 700,000 cycles, the vehicle camber was altered from  $-1^{\circ}$  to  $0^{\circ}$  to successfully reduce the rate of tyre wear.

Loading was halted after 1,000,000 cycles as per the brief. Although the pavement had not reached any of the pre-defined failure criteria, the rate of pavement deterioration (rutting) in both wheel paths had reached a stable state.

#### **3.6 Post-mortem**

The post-mortem analysis consisted of recording the condition of the pavement and excavating trenches across the width of the pavement to determine any changes in the properties of the different materials, and to attempt to determine the amount of rutting in each layer. Three trenches were excavated in each section, at locations corresponding to the minimum, average and maximum locations of pavement rutting.

Because of the requirements of the Transfund Project PR3-0504 (Increase in Mass Limits Effect on Pavement Wear – Stage 2) following on from this project, the trenches were not excavated until the completion of 1,325,000 vehicle passes. The primary reason for the delay in the trenching was to avoid disturbing the integrity of the pavement structure in the inner wheel path. However, one partial trench was excavated after 1,019,000 vehicle passes. This trench was located in Section A, in the outer wheel path at station 11.

Density measurements using the nuclear density meter were only undertaken on the surface on the asphalt. It was decided that, due to the disturbance of the surface materials if the excavations were carried out, the results from the density measurements would be unrepresentative of the undisturbed material. The moisture content of the subgrade material was measured by oven drying.

## 4. Results and Analysis

### 4.1 Materials Characterisation

The basecourse and subgrade materials were subjected to the following tests:

- Particle Size Distribution (PSD) tests (basecourse material only).
- Vibrating Hammer Maximum Dry Density (MDD) tests to determine the compaction and Optimum Moisture Content (OMC) targets.
- Repeat Load Triaxial testing (RLT) to determine the resilient modulus of the materials.

The PSD of basecourse materials was determined in accordance with NZS4407:1991 Tests 3.1, 3.8.1, 3.14 (SANZ 1991). The results from the PSD tests show that sections B and C materials have similar gradings in the sub-1.18mm sieve sizes, but they are significantly different at the bigger particle sizes. Also the maximum particle sizes are 20mm for the Australian material, and 40mm for the New Zealand materials. The PSD plots are shown in Figure 4.1, and the initial material that was used in section C is also shown in the plot. The percentage of fines in each material is shown in Table 4.1.

The maximum dry density tests were carried out using the NZS4402:1986 Test 4.1.3 method (SANZ 1986). The MDD and OMC values of the basecourse materials are shown in Table 4.2.

The RLT tests were carried out using the AS1289.6.8.1: 1995 test method (SA 1995) with two variations on the test procedure. The first variation was that the specimen size was 150mm x 300mm (diameter x height) and the standard uses 100mm x 200mm (DxH) specimens. The second variation was that the specimens were prepared at the field density and moisture content values rather than MDD and OMC values. The results are shown in Figure 4.2, where the resilient modulus is shown as a function of the bulk stress (the sum of the 3 principal stresses,  $\sigma_1 + 2\sigma_3$ ).

From Figure 4.2 it can be seen that materials B and C have similar resilient modulus values for the same test conditions. The fines contents of the two materials are similar (8% v 10%), but the maximum particle size (40mm v 20mm), particle shape (partially rounded, alluvial gravel v cubical quarried) and parent material are different.

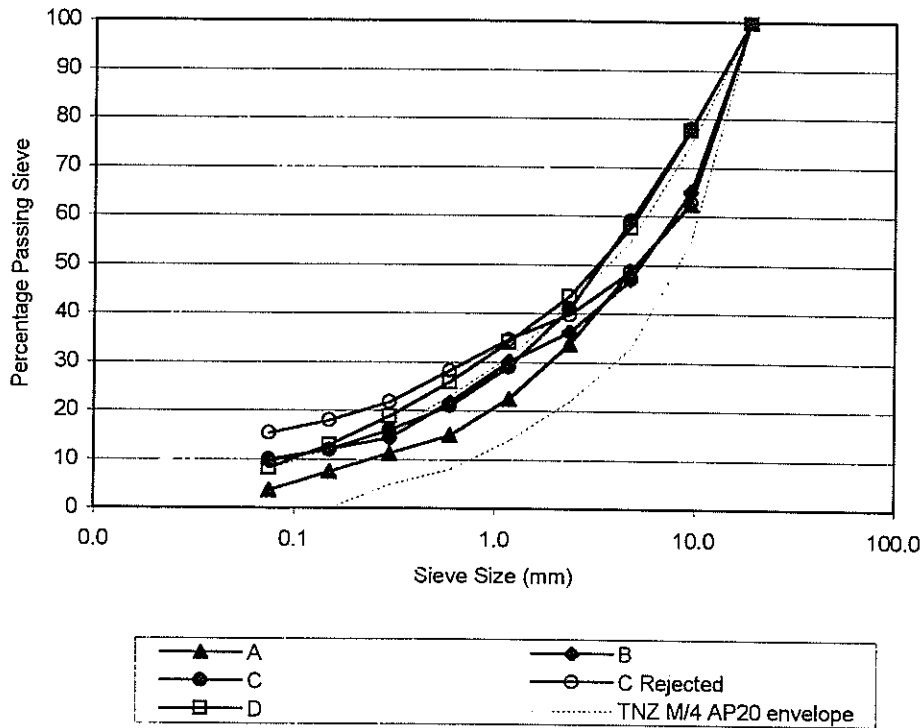


Figure 4.1 Particle Size Distributions for the basecourse materials.  
(note: the gradings have been scaled to 20 mm)

Table 4.1 Particle Size Distributions for the basecourse materials.

Material	Percentage passing 75 $\mu\text{m}$ sieve
A: Washed and crushed alluvial TNZ AP40 M4	3 (% of AP40 sample lot)
B: Crushed alluvial TNZ AP40 M4 with added fines	8 (% of AP40 sample lot)
C: Australian quarried AP20	10 (% of AP20 sample lot)
C Rejected: Crushed alluvial TNZ AP40 M4 with added fines	12 (% of AP40 sample lot)
D: Recycled concrete	7 (% of AP40 sample lot)

Table 4.2 Maximum Dry Density and Optimum Moisture Content values for the basecourse materials.

Material	MDD ( $\text{t}/\text{m}^3$ )	OMC (%)
A: Washed and crushed alluvial TNZ AP40 M4	2.32	6.0
B: Crushed alluvial TNZ AP40 M4 with added fines	2.36	4.8
C: Australian quarried AP20	2.26	6.0
D: Recycled concrete	2.12	10.5

#### 4. Results and Analysis

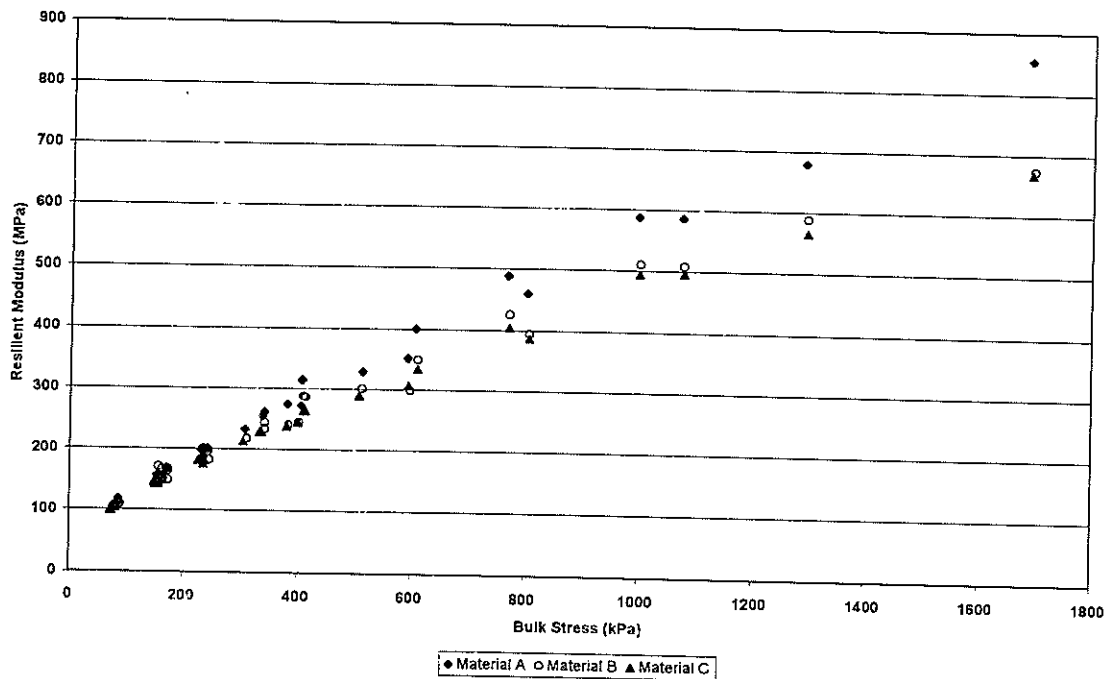


Figure 4.2 Resilient Modulus v Bulk Stress for the basecourse materials.

#### 4.2 Pavement Variability

In constructing a pavement at CAPTIF for a comparative study such as this, the aim is to minimise the transverse variability in the pavement structure so that the two SLAVE units are, as much as possible, trafficking identical pavements. Longitudinal variations in the pavement structure are less of a concern but it is difficult to construct a pavement that is very uniform transversely and irregular longitudinally. To test a parameter, such as layer thickness, for uniformity between the two wheel paths a new variable is constructed, which is the difference between the parameter's value on the inner wheel path and its value at a position on the same radial line in the outer wheel path. For a uniform pavement this new variable will have a mean equal to zero and a small standard deviation.

Tables 4.3 and 4.4 show the statistics of this difference variable for the asphalt and basecourse layer thicknesses respectively. At the 95% confidence level, if the range of the average difference  $\pm 2 \times$  standard error includes zero, then we cannot reject the null hypothesis that there is no difference between the inner and outer wheel paths. From Table 4.3 we can see that for the asphalt layer, only segment C shows no difference between the inner and outer wheel paths. For pavement segments A and B, the inner wheel path asphalt layer is approximately 5mm thicker than the outer wheel path, while for segment D, the outer wheel path is approximately 2mm thicker. The average asphalt layer thickness for the whole pavement is about 27mm.

Although the 5mm difference is a significant proportion of the overall layer thickness, thin-surface pavement design assumes that the asphalt layer does not contribute to the structural capacity of the pavement and so this should not impact significantly on the performance of the two wheel paths.

**Table 4.3 Difference (inner – outer wheel path) in asphalt layer thickness.**

Segment (Station No.)	Average (mm)	Minimum (mm)	Maximum (mm)	Standard Deviation (mm)	Range (mm)	Standard Error (mm)
A (0-15)	4.92	-1.38	14.25	4.13	15.63	1.03
B (16-29)	4.89	-3.00	10.38	3.74	13.38	1.00
C (30-43)	0.16	-4.75	6.13	3.45	10.88	0.92
D (44-57)	-1.79	-2.13	-1.25	0.47	0.88	0.27

**Table 4.4 Difference (inner – outer wheel path) in basecourse layer thickness.**

Segment (Station No.)	Average (mm)	Minimum (mm)	Maximum (mm)	Standard Deviation (mm)	Range (mm)	Standard Error (mm)
A (0-15)	5.13	-10.13	25.25	9.81	35.38	2.45
B (16-29)	-3.94	-15.75	11.25	7.59	27.00	2.03
C (30-43)	1.93	-8.00	9.88	4.76	17.88	1.27
D (44-57)	0.21	-1.25	2.25	1.82	3.50	1.05

From Table 4.4, which shows the analysis of the basecourse layer, Segments B, C and D have an average which is not significantly different from zero at the 95% confidence level. The average for Segment A is greater than zero but only just outside the 2 standard error confidence interval and, as the average thickness of the basecourse layer is 276mm, the difference is less than 2%. The basecourse layer is the main structural element in a thin-surface pavement and, to all intents and purposes, the inner and outer wheel paths have the same thickness basecourse layer.

During construction, Loadman Falling Weight Deflectometer measurements were taken at five transverse positions at twelve stations (three in each pavement segment) on the top of the subgrade layer. As the subgrade was identical for all four segments, we consider the difference function on this layer for the whole track. This was negative (average value  $-7\text{MPa}$  with a standard error of  $3.4\text{MPa}$ ). The average value for both wheel paths was  $68\text{MPa}$ , so the inner wheel path average was 10% below the outer wheel path. For the basecourse layers, readings were taken at nine stations (three in each of segments A, B and C). At the 95% confidence level, there was no significant difference in the readings between the two wheel paths either by segment or for the pavement as a whole. Experience with the Loadman at CAPTIF has shown the repeatability of the results to be approximately  $10\text{MPa}$ . Thus, based on the Loadman measurements, the inner and outer wheel paths appear to be identical.

### 4.3 Zero Measurements

Both vehicles were fitted with the same steel leaf spring suspension and no viscous dampers. For the test, vehicle A was loaded to 40kN and vehicle B was loaded to 50kN. A series of EC drop tests was undertaken to characterise the suspension response in the test load configuration. The results of these tests are detailed in Table 4.5. Although the two suspensions are identical, the natural frequency of the more heavily loaded vehicle is lower as is expected from the increased mass. Similarly the damping ratio is higher with increased mass.

**Table 4.5 Mean natural frequency and damping values.**

Load	Natural frequency (Hz)	Damping ratio (%)
Vehicle A (40kN load)	2.17	7.3
Vehicle B (50kN load)	1.81	8.8

The dynamic wheel forces were measured for both vehicles at the test speed of 45km/h travelling along the track centreline. These are shown in Figure 4.3. The lower natural frequency of vehicle B is clearly visible. Although vehicle B is generating higher dynamic loads it also has a higher static load. The most widely used way of characterising dynamic wheel loads is with a measure called the Dynamic Load Coefficient (DLC), which is defined as:

$$\text{DLC} = \frac{\text{Standard deviation (wheel force)}}{\text{Mean(wheel force)}}$$

Clearly if there are no dynamic wheel forces DLC is zero. The DLC values for the wheel forces shown in Figure 4.3 are both 0.11, so the relative level of dynamic loading generated by the two vehicles at the test speed on the same pavement was the same at the start of the test. Thus the fundamental difference in the loading applied by the two vehicles is in the magnitude of the static load, as the dynamic component is proportionately the same.

## 4.4 Test Measurements

### 4.4.1 Dynamic Wheel Forces

At every measurement interval the dynamic wheel forces were measured for both vehicles operating in the test wheel paths at the test speed of 45 km/h. Typically as the pavement roughness increases the DLC of the vehicles increases. In previous tests at CAPTIF (de Pont et al. 1999), DLC has proven to be a clearer indicator of increasing roughness than longitudinal profile measures such as IRI. Figure 4.4 shows the change in DLC with increasing load cycles. The results of the measurements at 600,000 load cycles have been omitted from this plot because they were inconsistent with the other results. This inconsistency was not discovered until data analysis commenced, and may have arisen from a problem with the measurement system during the testing. Because the problem was not obvious at that time, the reasons for the faulty data could not be determined.

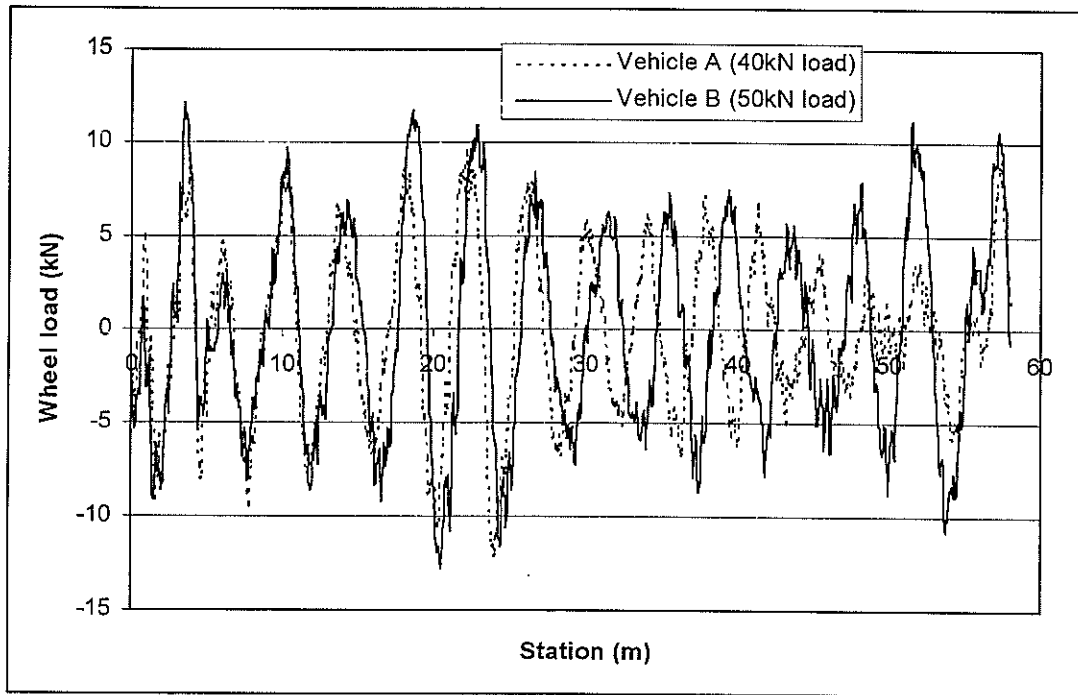


Figure 4.3 Dynamic wheel forces on the centreline at the start of the test.

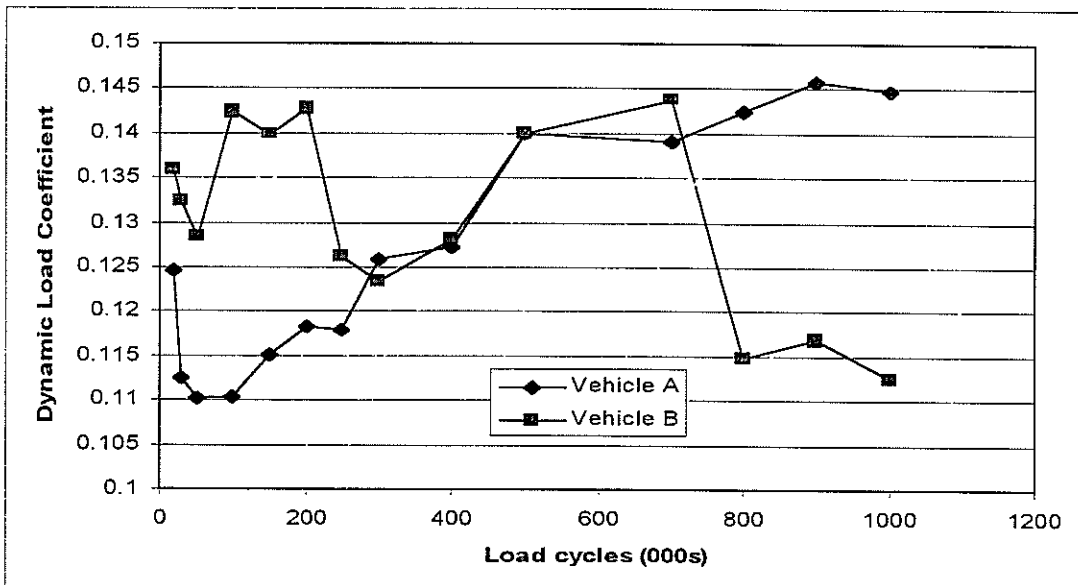


Figure 4.4 Change in DLC with increasing load cycles.



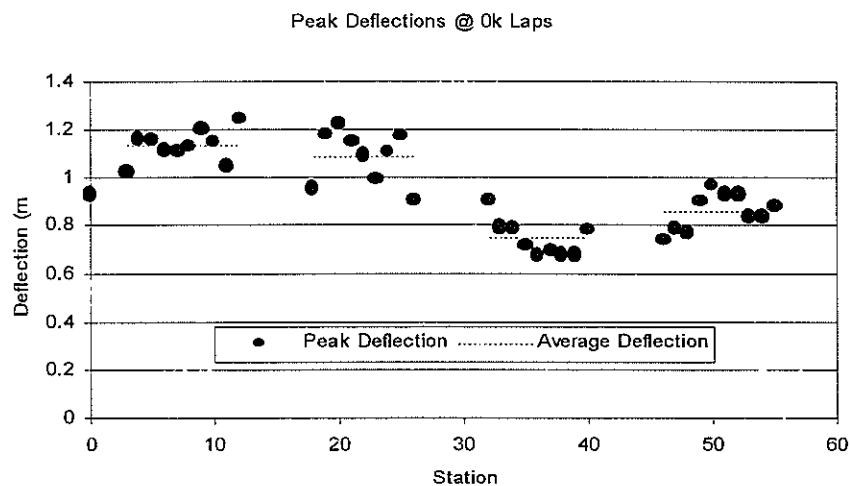
The DLC values for vehicle A, which was loaded to 40kN and operated on the inner wheel path, show the typical response for a CAPTIF test. Initially there is a reduction in DLC as the post-construction compaction smooths the pavement. Following this, a steady increase is seen in DLC as the pavement roughness increases. The behaviour of the DLC values for vehicle B, which was loaded to 50kN and operated in the outer wheel path, is more complicated. As with vehicle A, an initial reduction in DLC occurs, reflecting the post-construction smoothing of the pavement. This is followed by an upward trend in DLC until 200,000 load cycles when there is an abrupt reduction. Then again an increase is recorded up until 700,000 load cycles, where again an abrupt reduction is seen. These two sudden reductions in DLC correspond exactly with the seal-rehabilitation work undertaken in the outer wheel path, which was outlined in Section 3.5.

Although this rehabilitation explains the results of the DLC measurements well, it does mean that they would be difficult to use for any quantitative assessment of pavement performance.

#### 4.4.2 CAPTIF Deflectometer and FWD Measurements

On completion of construction, the CAPTIF deflectometer was used to measure the stiffness of the pavement. These measurements were made along the centreline of the track and thus do not identify differences between the inner and outer wheel paths. However, the earlier analysis of the layer thickness and Loadman measurements in Section 4.2 showed that the two wheel paths were substantially the same. The peak deflections measured by the CAPTIF deflectometer are shown in Figure 4.5.

Figure 4.5 Peak deflections measured by CAPTIF deflectometer at post-construction.



The four clusters of measurements, which are used to calculate the average values shown in the figure, correspond to the four pavement segments and are in alphabetical order from left to right. A higher peak deflection represents a lower elastic modulus and so, in order of increasing modulus, the pavement segments are ranked A, B, D, C with A and B quite similar and C and D also quite similar.

The final FWD results after the pavement was completed suggested that the pavement would fail just under 1 million cycles in the inner wheel under the 8.2 tonne axle load assuming the AUSTROADS subgrade strain criterion, suggesting that the pavement was not quite as strong as assumed in the design.

During the testing, FWD measurements were undertaken at each of the 58 stations around the track in both wheel paths after 30,000, 200,000, 600,000 and 1,000,000 load cycles. The average peak deflections by pavement segment are shown in Figure 4.6. The results for all of the pavement segments show a similar pattern of an initial increase then a decrease. After 30,000 load cycles there is already a significant difference between the inner and outer wheel paths. That is, the initial compaction that occurs immediately post-construction has resulted in differences in pavement stiffness between the inner and outer wheel paths.

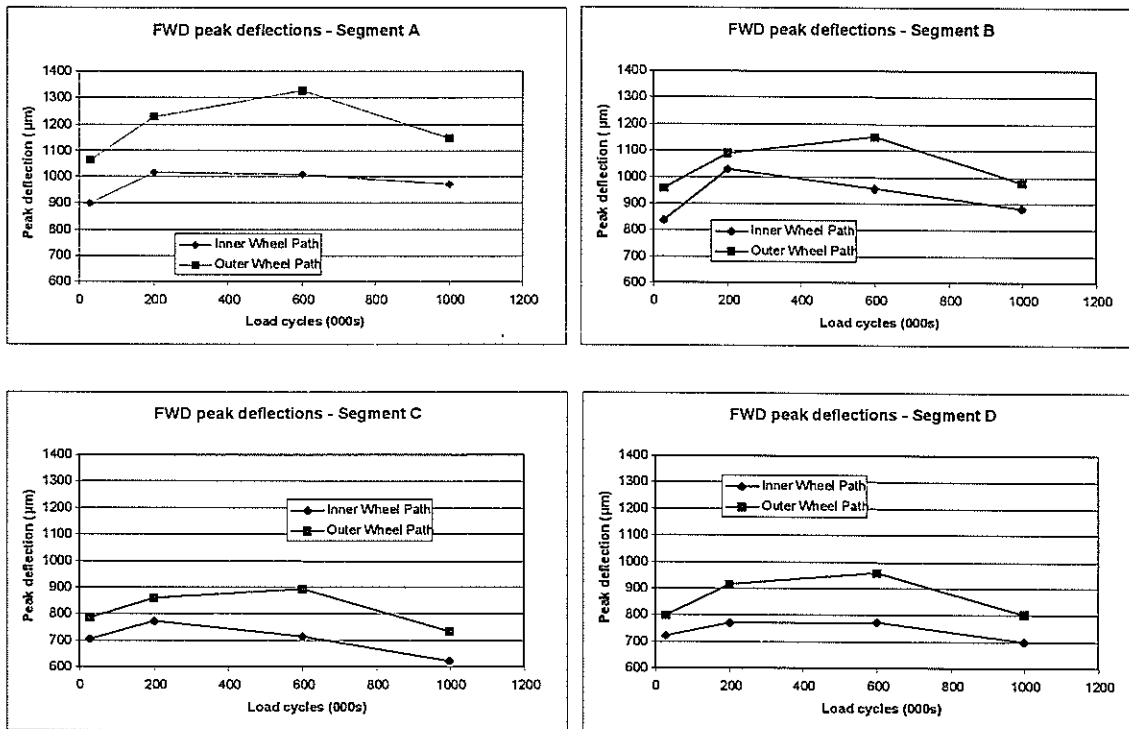


Figure 4.6 FWD average peak deflections by pavement segment.

During the next phase of loading, the stiffness of both wheel paths degrades further before stabilising and then improving. For all four pavement segments the inner wheel path, which was trafficked with the lighter load, begins increasing in stiffness sooner than the outer wheel path but the rate of increase for the outer wheel path is greater. It is not clear what the mechanism is that is generating this improvement in stiffness, but it does not appear to result in a reduction in the rate of wear of the pavement as is shown in Section 4.4.4.

#### **4.4.3 Longitudinal Profiles and Roughness**

Standard CAPTIF procedure is to determine the roughness of the pavement from the single laser profiler mounted on vehicle A. Measurements were taken throughout the project, which were based on the centreline of the two wheel paths. However the measurements have subsequently shown to be too variable to be used for detailed analysis. The reason for the high level of variability is that the profiles were measuring a line of pavement that was not trafficked during the loading phase. The distance between the tyres in the dual tyre assembly was 130mm, but the wheel path wander pattern was limited to  $\pm 50$ mm. This meant that there was a 30mm-wide section of pavement in the middle of the tyres that was not trafficked. This untrafficked section of pavement coincided with the centreline of the wheel paths.

#### **4.4.4 Vertical Surface Deformations and Rutting**

At each measurement interval the transverse profile of the pavement was measured at each station. For these measurements, the permanent vertical surface deformation (VSD) and the rut depth can be calculated. VSD has proved in past CAPTIF tests (de Pont et al. 1999) to be a fundamental measure of pavement wear that provides useful insights into the pavement performance and behaviour. Both rutting and surface roughness are related to VSD and so VSD reflects both these forms of pavement wear. Rutting is directly caused by VSD while roughness is caused by the variation in VSD. As VSD has been shown to be correlated to both dynamic wheel forces and the variability in pavement structure (de Pont et al. 1999), increasing VSD leads to increased roughness. With the transverse profiler at CAPTIF it is possible to measure VSD to a good degree of accuracy and reliability because the measurements are all referenced back to the edges of the concrete tank which are very stable.

Measurements of rutting and roughness do not have the same level of reliability (de Pont et al. 1999). Rutting is determined by calculating or measuring the depth of the rut from a straight edge laid across the wheel path. Thus the rut depth depends not only on the VSD in the centre of the wheel path but also that of the highest tangential points inside and outside the wheel path. Roughness is usually given in International Roughness Index (IRI) values, which are calculated from the longitudinal profile using the response of the simulated quarter car.

The dynamic characteristics of the quarter car are such that it responds to surface profile characteristics with wavelengths from 1m to 30m (Sayers et al. 1986). To accurately sample the longer wavelength components in this range, it is normally recommended that the section length for IRI calculation is greater than 100m. As the track at CAPTIF is only 58m long it does not meet this requirement.

Figures 4.7 and 4.8 show the progression of VSD for each of the wheel paths in each pavement segment. Note that as outlined in Section 3.5, parts of the pavement surface in the outer wheel path in segment C were repaired at 200,000 cycles and at 700,000 cycles.

The VSD values for these repaired sections were therefore meaningless, and so the average VSD for the outer wheel path of segment C is calculated from only those stations that had not been repaired. As this left only four stations out of fourteen it is expected that the variability will be greater for this dataset.

#### **4.4.5 Fitting a Power Law**

For all four pavement segments the VSD is greater on the outer wheel path, which was trafficked with the higher load than on the inner. The conventional approach to comparing the wear generated by two different axle loads is the power law method. This states that the amount of pavement wear caused by one pass of an axle is proportional to some power of its axle load. The most widely used value for this power is four. Thus if a given level of wear is achieved by  $N_{inner}$  load cycles of a load  $P_{inner}$  or by  $N_{outer}$  load cycles of a load  $P_{outer}$  these are related as follows:

$$\frac{N_{inner}}{N_{outer}} = \left[ \frac{P_{outer}}{P_{inner}} \right]^n$$

where  $n$  is the exponent of the power law

For every measured value of VSD and load cycles on the inner wheel path, the number of load cycles on the outer wheel path to generate the same VSD can be calculated by interpolation. Alternatively, the number of load cycles on the inner wheel path that are needed to generate the measured VSDs in the outer wheel path can be calculated.

In either case, as  $P_{inner}$  and  $P_{outer}$  are known, the value of the exponent,  $n$ , required to get the power law relationship to hold can be calculated for each VSD value.

Whether the inner or outer wheel path VSD measurements are used as the reference makes relatively little difference to the results. For segment A, the average exponent value was 8.9 using the inner wheel path VSDs as the reference, and 9.3 using the outer wheel path VSDs. For segment B, the corresponding values were 6.1 and 6.3, for segment C, 2.8 and 2.9, and for segment D, 3.8 and 3.9. Averaging across both sets of data gives exponents of 9, 6.2, 2.8 and 3.8.

4. Results and Analysis

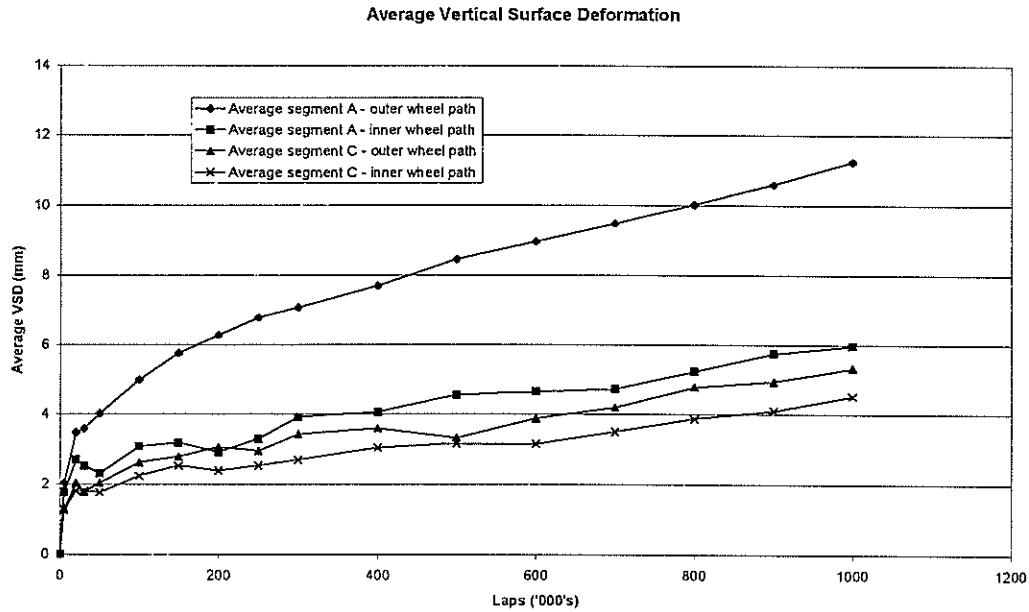


Figure 4.7 VSD for pavement segments A and C.

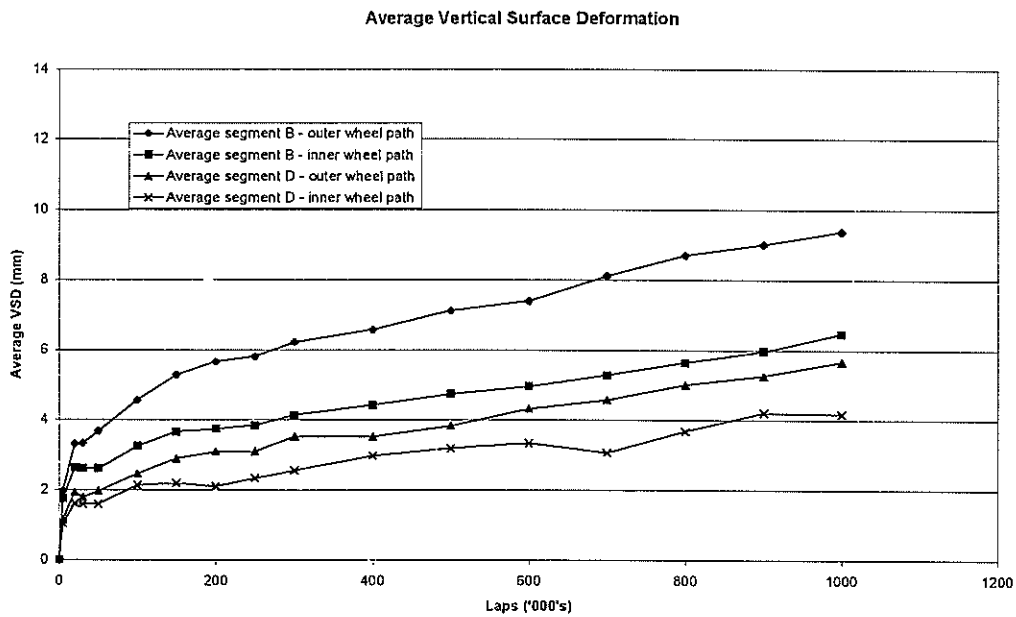


Figure 4.8 VSD for pavement segments B and D.

Using these values in a model gives a reasonable fit to the measured data. If 8.2 tonnes is used as a standard axle load, every load cycle on the inner wheel path corresponds to 1 “equivalent standard axle” or ESA. On the outer wheel path each load cycle would correspond to  $(10/8.2)^n$  ESA where  $n$  is the exponent calculated above. Thus for segment A, where the exponent is 9, 1,000,000 load cycles corresponds to 5,966,000 ESA. Figure 4.9 shows the power law fits for each of the

pavement segments. As can be seen, this form of model provides a reasonable although far from perfect fit to the data.

However, there are two major problems with this model. The first is that it does not explain why the rate of increase in VSD changes so much as the loading progresses, and the second is the wide variation in the value of the exponent between the different pavement segments. These four segments are all variations of a basic thin-surface pavement structure and yet the best-fit exponents for a power law model range between less than 3 and 9.

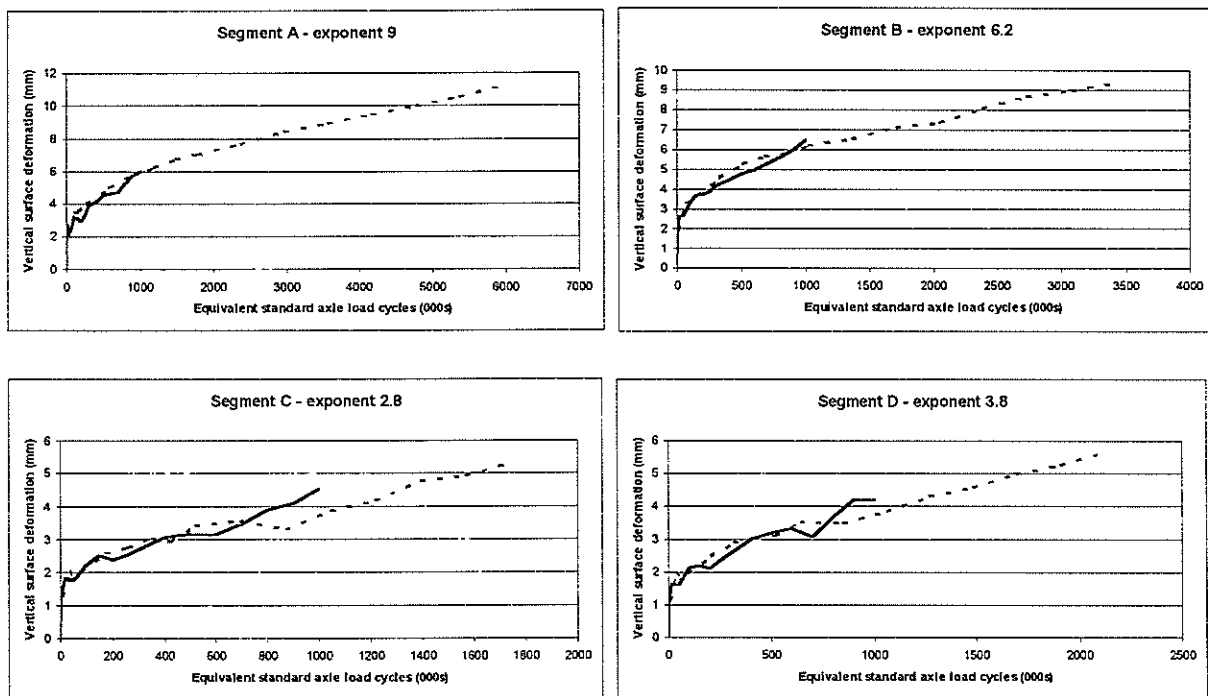


Figure 4.9 Power law fits to VSD for all four segments.

Looking again at Figures 4.7 and 4.8, VSD is seen to increase rapidly during the initial loading cycles and then slow to a linear rate of increase. This suggests that the VSD consists of two components, an initial post-construction compaction and then a wear-related component. If a straight line is fitted to the linear part of the VSD versus load cycles curve, then the intercept of this line with the vertical axis gives the post-construction compaction component and the slope of the line gives the wear-related component. The power law approach can then be used to compare both the intercept and the slope of these lines between the inner and outer wheel path for each segment.

4. *Results and Analysis*

**Table 4.6 Linear fit parameters for VSD v load cycles on inner wheel path.**

Segment	Intercept – Compaction (mm)	Slope – Wear rate (mm/1000 load cycles)	Goodness of fit – r <sup>2</sup>
A	2.74	0.00321	0.960
B	3.07	0.00327	0.993
C	1.91	0.00245	0.965
D	1.86	0.00233	0.904

**Table 4.7 Linear fit parameters for VSD v load cycles on outer wheel path.**

Segment	Intercept – Compaction (mm)	Slope – Wear rate (mm/1000 load cycles)	Goodness of fit – r <sup>2</sup>
A	5.37	0.00586	0.998
B	4.68	0.00480	0.993
C	2.24	0.00299	0.934
D	2.30	0.00332	0.986

Tables 4.6 and 4.7 show the results of a least squares regression straight line fit to the linear portions of the VSD v load cycles curves for each of the four segments in both wheel paths. As can be seen from the r<sup>2</sup> statistics, these are very good fits.

A power law fit can be applied to the compaction and wear components independently. This power law approach implies relationships of the form:

$$\frac{\text{Intercept}_{\text{outer}}}{\text{Intercept}_{\text{inner}}} = \frac{\text{Compaction}_{\text{outer}}}{\text{Compaction}_{\text{inner}}} = \left( \frac{\text{Axle load}_{\text{outer}}}{\text{Axle load}_{\text{inner}}} \right)^n \text{ where } n \text{ is the exponent of the power law}$$

$$\frac{\text{Slope}_{\text{outer}}}{\text{Slope}_{\text{inner}}} = \frac{\text{Wear}_{\text{outer}}}{\text{Wear}_{\text{inner}}} = \left( \frac{\text{Axle load}_{\text{outer}}}{\text{Axle load}_{\text{inner}}} \right)^n \text{ where } n \text{ is the exponent of the power law}$$

By taking logarithms, the values of n can be calculated for compaction and wear for each of the pavement segments. The results for the exponent values are shown in Table 4.8. It is interesting to note how similar the exponents are for the two components of VSD. The exponents for the different segments, while still not identical, are much more alike than they were in the simple power law model, particularly if segment C is discounted. Recall that a number of stations in the outer wheel path of segment C were repaired during the test and that the data from these stations were removed from the analysis leaving only four valid stations.

**Table 4.8 Exponent values relating compaction and wear between the inner and outer wheel paths.**

Segment	Intercept – Compaction	Slope – Wear rate
<b>A</b>	3.40	3.04
<b>B</b>	2.13	1.94
<b>C</b>	0.79	0.99
<b>D</b>	1.06	1.77

This model implies that the compaction is dependent only on the applied wheel load and not on the number of applications of this load (although a number of applications of the load are required to effect the compaction). The wear component is related to both the load and the number of load cycles. A logical extension to this model is that, if after some large number of load cycles the wheel load is increased, the additional compaction associated with the higher wheel load would then take place, as well as the higher rate of wear associated with a higher wheel load. The conventional power law approach does not predict an additional compaction with an increase in wheel load, only a higher wear rate.

Although this hypothesis was not tested explicitly because the test was completed before this analysis was done, a series of higher load cycles was applied to the inner wheel path after the completion of this test as part of another project. VSD measurements were taken as part of that project and the results are shown in Figure 4.10. The project being reported here was finished at 1,000,000 load cycles. The subsequent project involved looking at the strain response of the pavement under various loading conditions, which included loads 40kN, 50kN and 60kN with varying tyre pressures and on both wide single and dual tyres. Thus a direct assessment of the expected wear impact is difficult to make. However, the change in VSD after 1,000,000 load cycles does appear to reflect an additional compaction rather than just a change in wear rate.

Previous work at CAPTIF on the impact of dynamic loading on pavement wear (de Pont et al. 1999) also found a power law relationship for wear rate that had a relatively low exponent (between 1 and 2). This fits in well with exponent values found for this compaction and wear model, and not with the higher powers normally associated with a power law model.

Note that the terms “compaction” and “wear” to describe the two components of VSD are not based on any knowledge of the underlying material behaviour. Previous measurements by Patrick et al. (1998) measuring the density of in-service pavements found no significant increase in basecourse density during this post-construction compaction phase. Further investigation is needed to determine the mechanism generating the behaviour.



4. Results and Analysis

If this model is correct, there are significant implications for road controlling authorities particularly if a change in axle load limit occurs. The wear rate will increase according to a power law with an exponent between 1.8 and 3. This means that, if the axle load limit is raised by 7.3% as suggested, the wear rate per axle for those axles at the higher loads will increase by between 13.5% and 23.5% depending on which exponent value is used. As road user charges are based on a fourth power law, the increase in wear component of road user charges will be 32.5% for the higher loaded axles and thus will more than offset the additional wear.

However, the compaction component also has an exponent of between 1 and 3.4. Increased axle loads will therefore also cause an additional one-off compaction of the pavement across the whole network. For a 7.3% axle load increase, this will be between 7.3% and 27% of the compaction that occurred initially on the pavement after construction. For the four pavement segments tested here, the magnitude of the initial compaction was equivalent to the wear induced by between 700,000 and 980,000 load cycles. Thus an increase in axle load limit of 7.3% would lead to an increase in VSD due to compaction which is equal in magnitude to the wear-related VSD associated with between 50,000 and 265,000 load cycles.

For a typical New Zealand State Highway, the average heavy vehicle traffic is around 100 vehicles/day. Assuming the average vehicle applies about 3 ESA implies about 100,000 standard axle loads per year. Thus increasing the axle load limit by 7.3% will result in an additional compaction that is equivalent to between 6 months and 2½ years of normal loading. This additional VSD would occur in a relatively short period, probably less than a year, of the change.

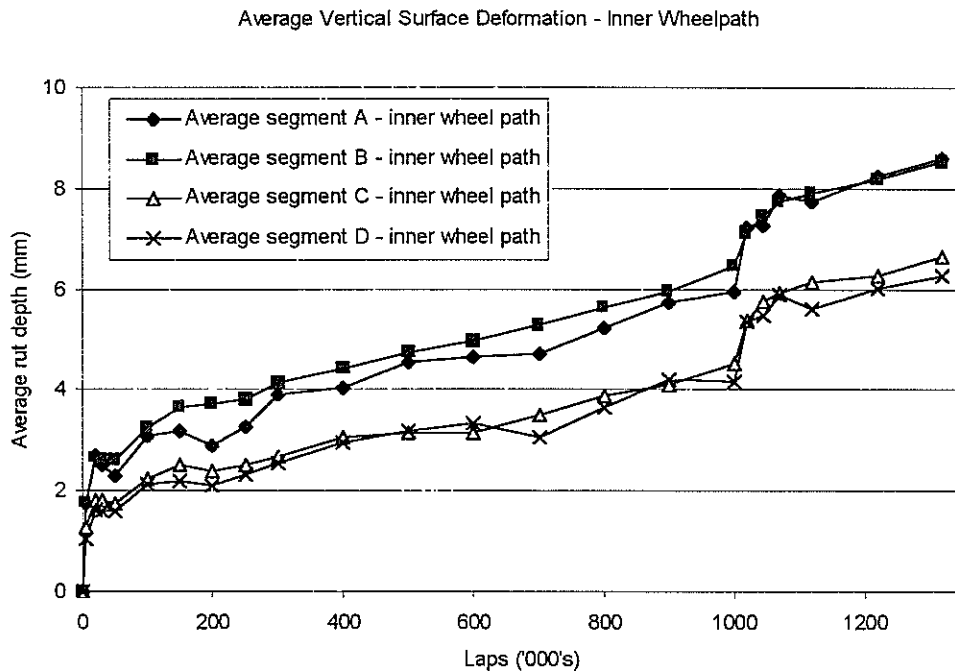


Figure 4.10 VSD v load cycles for inner wheel path.

#### 4.5 Post-mortem Measurements

At the end of testing, nine trenches were excavated at various stations around the track. Three trenches were located in each of the three different pavement sections. The locations of the trenches are shown in Table 4.9 and Figure 4.11. The manual profile beam was used to measure the surface profile of the asphaltic concrete surface layer at each of the selected stations, and then the asphaltic concrete was cut with a saw and removed to expose the surface of the basecourse material. In some locations, some of the basecourse material adhered to the bottom of the asphaltic concrete. This made it impossible to accurately determine the surface profile of the basecourse material at these locations. An excavator was used to remove most of the basecourse material from the trenches, but the bottom 50mm or so of granular material was carefully removed by hand so that the surface of the subgrade was not disturbed. The surface profile of the subgrade was measured with the manual profile beam.

The thickness of the asphaltic concrete and basecourse layers before and after trafficking was determined by calculating the difference between the profile measurement at the top and bottom of each layer. The accuracy of the measurements was checked by comparing the change in thickness of the asphaltic concrete layer in the untrafficked regions of the pavement. The measurements showed that the thickness of the untrafficked regions of the surfacing layer had decreased at one of the points, remained the same at nine points, and increased at 47 points. For the points that had increased in thickness during the test, the average, maximum and minimum increases in layer thicknesses were 3.4, 10, and 1mm respectively, with a measurement resolution of 1mm.

These results show the difficulty in determining, with any degree of accuracy and confidence, the surface profile of the basecourse. This difficulty is primarily caused by basecourse particles adhering to the bottom of the asphaltic concrete layer. The adhesion of particles is caused by the application of a tack coat during pavement construction. The tack coat is a bitumen emulsion that is sprayed onto the surface of the basecourse before the laying of the asphaltic concrete surfacing layer. The purpose of the tack coat is to enhance the bond between the basecourse and asphaltic concrete layers. For this reason, the measurements taken on the surface of the basecourse material have not been used in the rutting calculations, and the asphaltic concrete and basecourse layers are treated as single layer. It is assumed that most of the rutting in this combined layer occurs in the basecourse material, as this material accounts for 92% of the layer thickness (25mm v 275mm).

Because of the requirements of Transfund Project PR3-0504 (Increase in Mass Limits Effect on Pavement Wear – Stage 2) that followed on from this project, the trenches were not excavated before the completion of 1,325,000 vehicle passes. The primary reason for the delay in the trenching was to avoid disturbing the integrity of the pavement structure in the inner wheel path. However, one partial trench was excavated after 1,019,000 vehicle passes. This trench was located in Section A, in the outer wheel path at station 11.

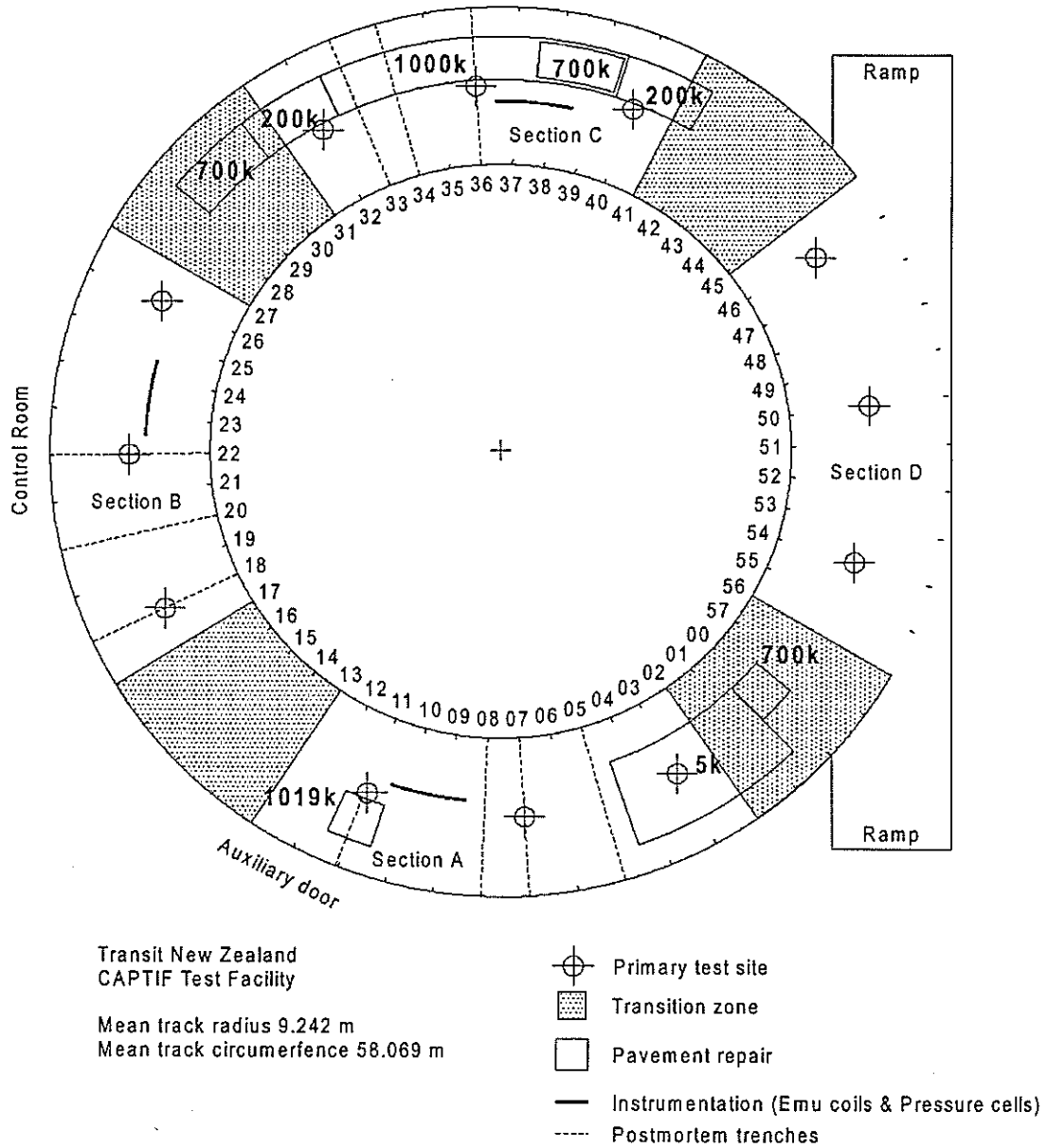


Figure 4.11 Plan showing the locations of the post-mortem trenches and surfacing repairs.

Table 4.9 Locations of the post-mortem trenches.

Test Section	Station	Reason for selection
A – “Clean” TNZ M4 AP40	5	Maximum rut depth
	7	Average rut depth
	8	Minimum rut depth
B – “Dirty” TNZ M4 AP40	18	Maximum rut depth
	20	Average rut depth
	22	Minimum rut depth
C – Australian AP20	33	Maximum rut depth
	34	Average rut depth
	36	Minimum rut depth

The results of the partial excavation at station 11 are shown in Figure 4.12. Analysis of the data shows that the rutting in the subgrade and basecourse materials was 6.0 and 3.3mm respectively (64%, 36%). The total rut depth was 9.3mm. The trench profiles from the nine trenches excavated after 1,325,000 cycles are shown in Appendix A. The total rut depth and percentage of rutting in the basecourse and subgrade materials are shown in Table 4.10. The profile data has been averaged over the range 1100–1600mm and 2200–2700mm for the inner and outer wheel paths respectively. Overall, the trench data shows that 42% of the rutting occurred in the subgrade material and 58% occurred in the basecourse and asphalt layers.

The measurement of the surface density of the pavement with a nuclear density gauge showed no significant difference between the density of the new pavement and the trafficked pavement. The average density in the inner wheel path increased from 2093 to 2118kg/m<sup>3</sup> and the density in the outer wheel path increased from 2090 to 2091kg/m<sup>3</sup>. In both cases the change is within the repeatability limits of the measurement device.

A visible difference was noted in the performance of the asphalt surfacing under the two wheel loads: section A cracked in the outer wheel path only; section B cracked in both wheel paths, although the outer wheel path was more heavily cracked; and section C cracked in the outer wheel path, and all but 5m of the asphalt surfacing was replaced during the testing. The failure of the surfacing that was replaced appeared to related to a lack of bonding between the asphalt and the basecourse surface, which caused the surfacing to tear or shove. The surfacing appeared to have trouble coping with the heavier wheel load.

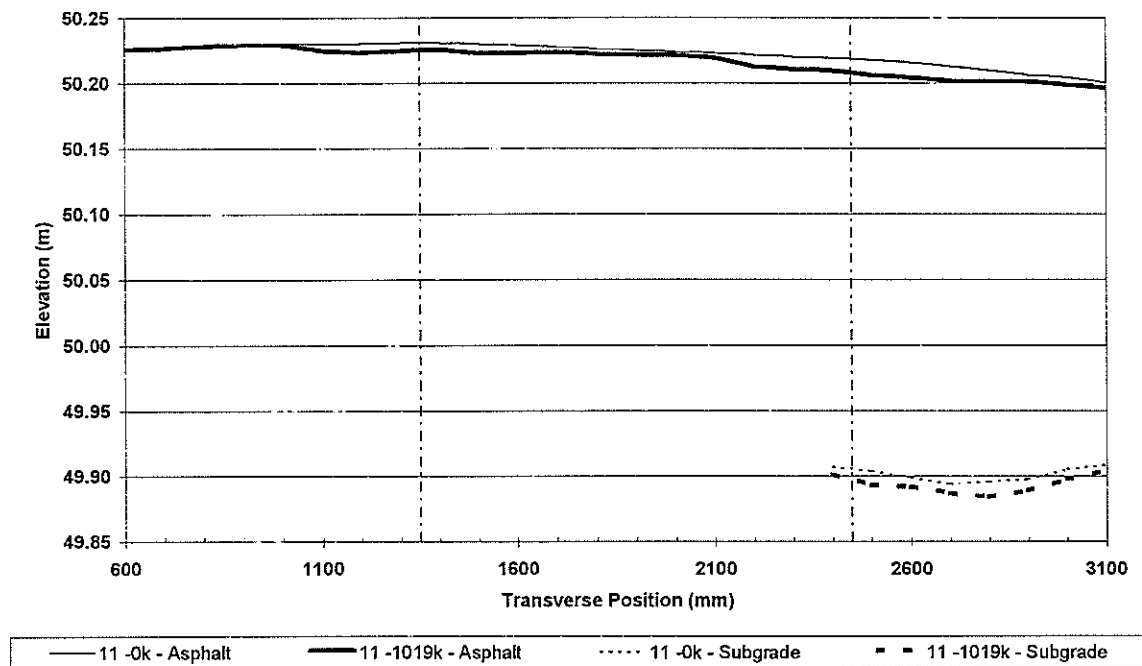


Figure 4.12 Trench profile for station 11 after 1,019,000 cycles.

Table 4.10 Rut data for the post-mortem trenches.

Station	Inner Wheel path					Outer Wheel path				
	Subgrade		Basecourse		Total	Subgrade		Basecourse		Total
	Value (mm)	% of Total	Value (mm)	% of Total	Value (mm)	Value (mm)	% of Total	Value (mm)	% of Total	Value (mm)
5	2.0	27	5.3	73	7.3	0.2	2	7.3	98	7.5
7	4.2	63	2.5	38	6.7	3.5	28	8.8	72	12.3
8	2.8	53	2.5	47	5.3	6.3	81	1.5	19	7.8
18	3.3	42	4.7	58	8.0	1.8	31	4.2	69	6.0
20	3.7	49	3.8	51	7.5	7.5	57	5.7	43	13.2
22	1.8	30	4.3	70	6.2	2.5	31	5.7	69	8.2
33	0.0	0	6.5	100	6.5	1.7	53	1.5	47	3.2
34	-1.2	-22	6.5	122	5.3	2.7	229	-1.5	-129	1.2
36	-4.3	-93	9.0	193	4.7	1.5	113	-0.2	-13	1.3

Note: these values are the average values over the respective wheel paths.

#### 4.6 Discussion

The key results of this test are those relating to the VSD analysis found in Section 4.4.4. VSD is a fundamental measure of the pavement's performance and relates directly to both rutting and roughness. Although conventional power law relationships can be fitted to these results, they are not very satisfactory because, even though the four pavement segments tested are of similar design type, the exponents of the best fit power laws vary tremendously from segment to segment. The reason for this is that the VSD appears to consist of two components:

1. an initial compaction component, which is primarily related to the applied load and not to the number of loading cycles; and
2. a wear-related component, which is related to both load and number of load cycles.

Fitting a conventional power law relationship to the whole VSD history requires part of the compaction component for the more heavily loaded wheel path to be matched by part of the wear-related component in the more lightly loaded wheel path. This results in some high exponent values.

By treating these two components separately, a power law relationship can be fitted to each independently. Surprisingly the exponents for the two components are remarkably similar for each pavement segment. Although there is still some variation in exponents between pavement segments, this is much less than it was for the conventional power law fits. Support for the validity of this model is found in the behaviour of the pavement after the completion of the test, when some further tests with higher loads were undertaken on the inner wheel path. It appears that the compaction associated the higher loads still occurred at this time even though the pavement had already been subjected to 1,000,000 load cycles at a 40kN wheel load.

The implication of this is that, if an increase in axle load limit occurred, there would be an immediate rapid increase in VSD that would manifest itself as an increase in rutting and roughness due to additional compaction of the pavements. The long-term effect would be an increase in wear rate proportional to a second or third power of the axle loads. The additional road maintenance costs of this long-term effect would be more than covered by road user charges, which are based on a fourth power relationship.

In fact, there are some grounds for revising the road user charges schedule to reflect the lower powers. However, the short-term increased compaction would require substantial additional pavement maintenance over the first year or two to maintain the performance of the highway network. For example, if the compaction was equivalent to six months wear (as calculated in Section 4.4.4) then, over the first two years after the change, 150% of the current annual budget for roughness and rutting rehabilitation would need to be spent.

## 5. Conclusions

The aim of this study was to compare the pavement wear generated by a 10 tonne axle load with that of a standard 8.2 tonne axle with a view to predicting the cost implications of a change in the legal axle load limit for New Zealand highways. A pavement was tested at CAPTIF, which comprised four distinct segments, each of which was similar in design but utilised a different basecourse material. One of the SLAVE units at CAPTIF was configured to generate a 40kN wheel load (equivalent to an 8.2 tonne axle) and the other was configured for a 50kN wheel load (equivalent to just over a 10 tonne axle load). The two SLAVEs were then used to apply 1,000,000 load cycles to parallel wheel paths on the pavement. During the testing, measurements were taken to record the pavement wear, the pavement condition, the pavement response to the vehicle loading, and the vehicle response to the pavement.

From these measurements a number of important findings can be deduced:

- VSD, which is a fundamental form of pavement wear that results in both rutting and increased surface roughness, again proved to be the most useful measure for monitoring pavement wear at CAPTIF.
- Although a conventional power law relationship could be fitted to describe the differences in VSD between the two levels of loading for each of the four pavement segments, there was a large variation (between 2.8 and 9) in the exponent value required to give the best fit. As the pavement design of the four segments was substantially similar in character, it does not seem reasonable that the exponents for a power law model should vary so much. The variation also makes it impossible to predict the appropriate exponent value in advance. Thus the power law approach does not appear to be an accurate or useful way of modelling the VSD wear of this type of pavement.
- Reviewing the progression of VSD with load cycles shows that the pavement underwent two distinct phases of VSD. An initial period of rapid change was observed, here called compaction, followed by a period with a constant (linear) rate of change, called wear. Least squares regression can be used to fit a straight line to the linear part of the VSD versus load cycles curve. The intercept of this line with the y-axis then gives the compaction component, and the slope gives the wear.

For each of the four pavement segments, a power law can be used to relate the compaction and wear between the normally and more heavily loaded wheel paths. Remarkably, the best-fit exponent values for compaction and wear were quite similar for each pavement segment and did not vary too much between segments.

- This compaction-wear model implies that the compaction depends only on the magnitude of the applied load and not on the number of load cycles, while the wear depends on both the load and the number of load applications. A corollary of this is that, if the axle load level is increased at any stage, further compaction will occur to reflect this higher load.

As this model was developed well after the completion of the testing programme, this hypothesis was not specifically tested for, but in the project that followed this one at CAPTIF, the same pavement was used and higher loads were applied to the more lightly loaded wheel path. In this follow-up, the VSD did show an apparent increased compaction as would be expected.

- The exponent values for the compaction-wear model were between 1 and 3.4 for compaction and 1.8 and 3 for wear. (The values for pavement segment C were a little lower than this but repairs to the pavement surface during the test meant that very few data points could be used for this segment.) The implication of this is that, if the axle load limit were increased, the underlying wear rate of the compaction-wear model would increase as indicated by a power of between 1.8 and 3.

As the road user charges paid by these vehicles are based on a conventional model with a power of 4, the additional road user charges would more than offset the additional wear. In fact, there is some ground for considering a review of the road user charges schedule. But note that the effect of the compaction phase will also be observed in new construction and rehabilitation so this effect cannot be ignored, and an increase in axle load limit would also cause an immediate (over a year or two) additional compaction. Thus it would appear that the network had suddenly deteriorated substantially. This is a one-off effect but would need to be planned for by the road controlling authorities if pavement condition is to be maintained. If the road controlling authorities are not anticipating this additional compaction effect, the sudden apparent additional deterioration of the network will cause them great concern over the future maintenance demands.

- The existing fourth power approach is based on a chord approach, i.e. the amount of damage is considered only at the initial and terminal conditions. This research has shown that some merit may be gained in looking at a secant (tangential) rate of damage, but this approach would be difficult to incorporate into a charging model.
- Measurements of dynamic wheel force and pavement roughness showed qualitative trends that were as expected. However, as parts of the surface of the outer wheel path in segment C were substantially repaired at 200,000 load cycles and at 700,000 load cycles, any meaningful quantitative results could not be extracted from measurements that were taken for a complete circuit of CAPTIF.
- FWD measurements were taken at four intervals during the test. The results for the four pavement segments were very consistent with each other. In the early stages of the test there is a relatively rapid increase in peak deflection indicating a reduction in stiffness of the pavement. This rate of increase slows and by the end of the test is negative, indicating that the stiffness of the pavement is increasing slowly. In all four cases, the changeover from decreasing stiffness to increasing stiffness occurs sooner on the inner wheel path, which was trafficked with the lighter load.
- If the current conventional fourth power law approach is retained, then for New Zealand materials the power law should be increased, subject to the results obtained in the 2001/2002 experiment which will examine the power laws in a wider range of conditions.



## 6. Recommendations

From these findings a number of questions requiring further investigation arise:

- Further validation of the compaction-wear model is required. It is recommended that, in future CAPTIF trials where a wheel path has been trafficked with a constant load, after completion of the test some relatively small number (perhaps 300,000) of load cycles with a higher load are applied. If the compaction-wear model is valid, it will be possible to predict and test the amount of compaction that will occur. Work in progress at CAPTIF (2001) has attempted to address this issue but additional validation will be required.
- Although the compaction-wear model provides a good fit to the observed behaviour and is a useful predictor tool, the mechanisms underlying it are not understood. Further research is required to determine how the pavement materials are behaving and what is leading to the compaction and wear components of VSD. Note that the names, “compaction” and “wear”, are speculative and not based on any real knowledge of the underlying material behaviour.
- The FWD measurements indicate some rather interesting behaviour with the pavement stiffness increasing in the later stages of the test. This needs further investigation as it implies that, after an initial reduction, the structural capacity of the pavement increases with additional load cycles.
- More detailed analysis of the cost implications of the compaction-wear model are needed. The underlying wear rate of the compaction-wear model appears to be related to load by a power lower than four. However, the compaction component is also related to load by a power law.
- The VSD associated with compaction is equivalent to the wear associated with a considerable number of load cycles. If this compaction can be induced without causing rutting or roughness, the performance of the pavement would be enhanced considerably.
- The performance of thin asphaltic concrete surfacings under the higher axle loads needs to be investigated further. The pavement surfacing exhibited distress and failures under the 50kN axle load, but not under the 40kN axle load.

Overall the most significant finding of this study is the development of the compaction-wear model for VSD. This provides a much better fit to the observed behaviour than the conventional power law model, and has very significant implications for pavement management practice in New Zealand, and wherever thin-surface unbound pavement structures are widely used. The implication of the model is that, if an increase in axle load limit occurred, there would be an immediate rapid increase in VSD that would manifest itself as an increase in rutting and roughness due to additional compaction of the pavements.

The long-term effect would be an increase in wear rate proportional to a second or third power of the axle loads. However, the short-term increased compaction would require substantial additional pavement maintenance over the first year or two to maintain the performance of the road network. For example, if the compaction was equivalent to six months wear (as calculated in Section 4.4.4), then over the first two years after the change, 150% of the current annual budget for roughness and rutting rehabilitation would need to be spent.

Further validation work should be undertaken as well as research to understand the material behaviour mechanisms that produce this behaviour.

## 7. References

Arnold, G., Alabaster, D.A., Steven, B.D. 2001. Prediction of pavement performance from repeat load tri-axial tests on granular materials *Transfund New Zealand Research Report* (in press).

AUSTROADS. 1992. *Pavement design: A guide to the structural design of road pavements*. AUSTROADS, Sydney, Australia.

Cebon, D. 1999. *Handbook of vehicle-road interaction*. Swets & Zeitlinger, Lisse, Netherlands.

Council of the European Communities. 1992. *Annex III of the Council Directive 92/7/EEC amending Directive 85/3/EEC on the weights, dimensions and certain technical characteristics of certain road vehicles*. Council of European Communities, Brussels.

de Pont, J. 1997. OECD DIVINE project - Element 1. Longitudinal pavement profiles. *Industrial Research Limited IRL Report No.708*.

de Pont, J., Steven, B., Pidwerbesky, B. 1999. The relationship between dynamic wheel loads and road wear. *Transfund New Zealand Research Report No. 144*. 88pp.

Kinder, D.F., Lay, M.G. 1988. Review of the fourth power law. *Australian Road Research Board ARRB Internal Report MR 000-248*.

OECD. 1998. Dynamic interaction between vehicles and infrastructure experiment (DIVINE). *OECD Technical Report IRKD 899920*.

Patrick, J.P., Alabaster, D.J., Dongol, D.M.S. 1998. Pavement density. *Transfund New Zealand Research Report 100*.

Pidwerbesky, B.D. 1995. Accelerated dynamic loading of flexible pavements at the Canterbury accelerated pavement testing indoor facility. *Transportation Research Record 1482: 79-86*.

Pidwerbesky, B.D. 1996. Fundamental behaviour of unbound granular pavements subjected to various loading conditions and accelerated trafficking. *University of Canterbury Research Report 96-13*.

Sayers, M.W., Gillespie, T.D., Paterson, W.D. 1986. Guidelines for conducting and calibrating road roughness measurements. *World Bank Technical Paper 46*.

SA (Standards Australia). 1995. Soil strength and consolidation tests – Determination of the resilient modulus and permanent deformation of granular unbound pavements. *AS1289.6.8.1:1995*.

SANZ (Standards Association of New Zealand). 1986. Methods of testing soils for civil engineering purposes. Soil compaction tests. *NZ4402:1986 Test 4.1.3.*

SANZ. 1991. Methods of sampling and testing road aggregates. Laboratory tests. *NZ4407:1991 Tests 3.1, 3.8.1, 3.14.*

## Appendix A Graphs of Post-mortem Trenches

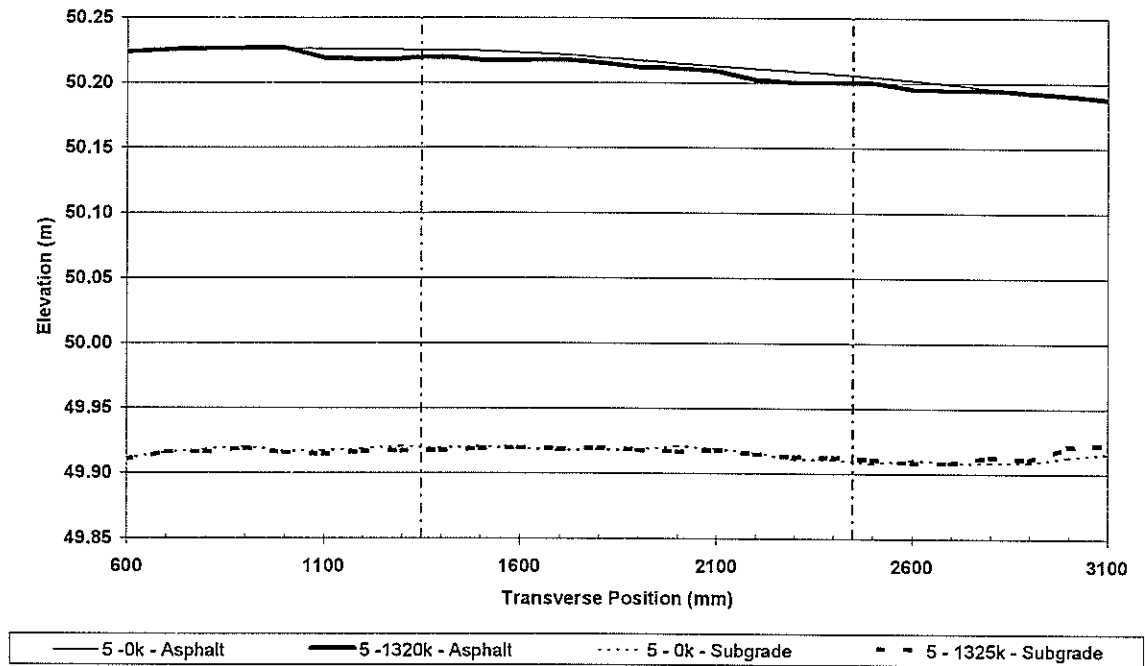


Figure A1 Section A post-mortem trench at station 5.

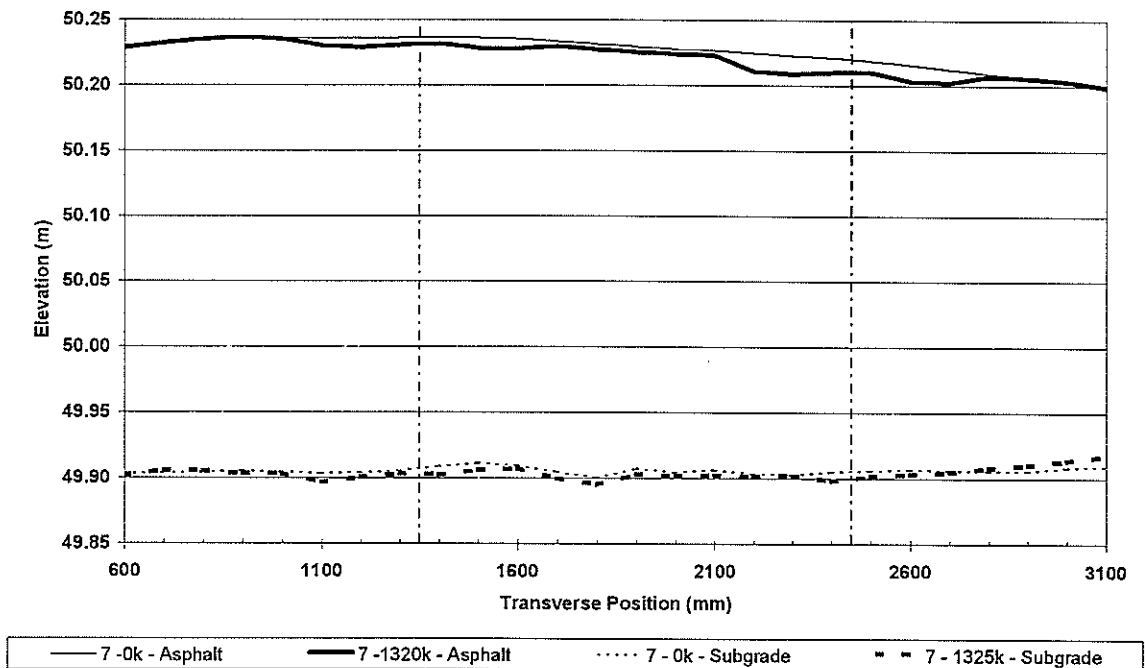


Figure A2 Section A post-mortem trench at station 7.

EFFECT ON PAVEMENT WEAR OF AN INCREASE IN MASS LIMITS

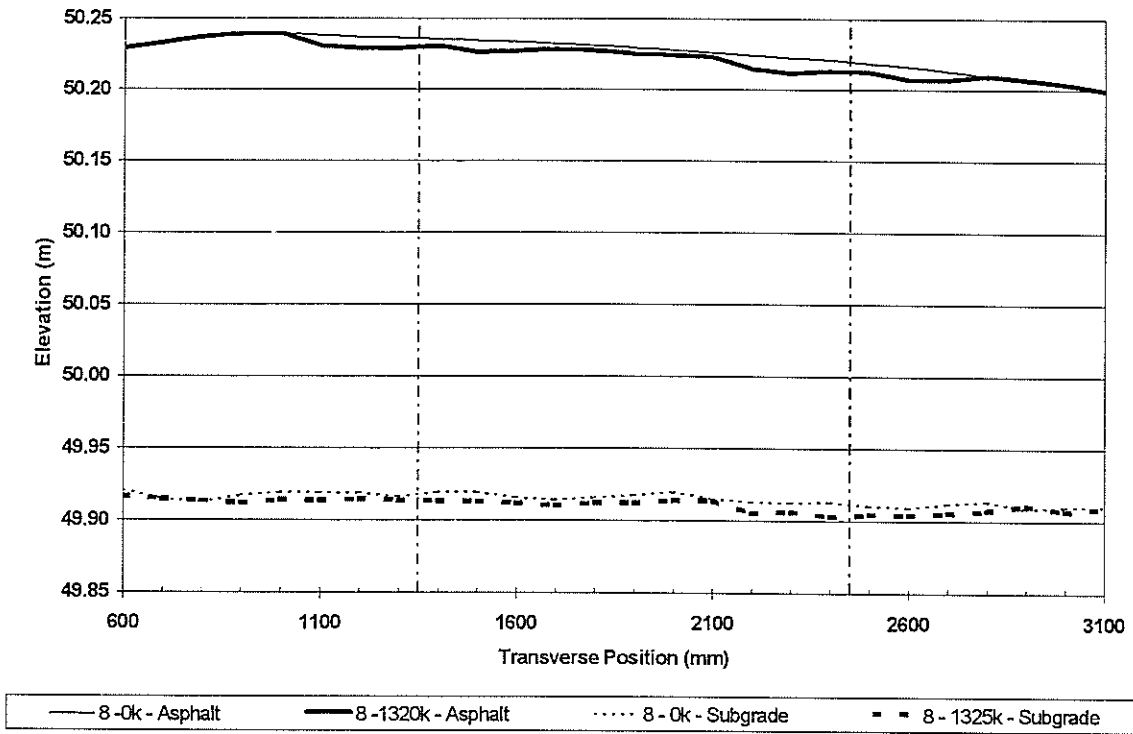


Figure A3 Section A post-mortem trench at station 8.

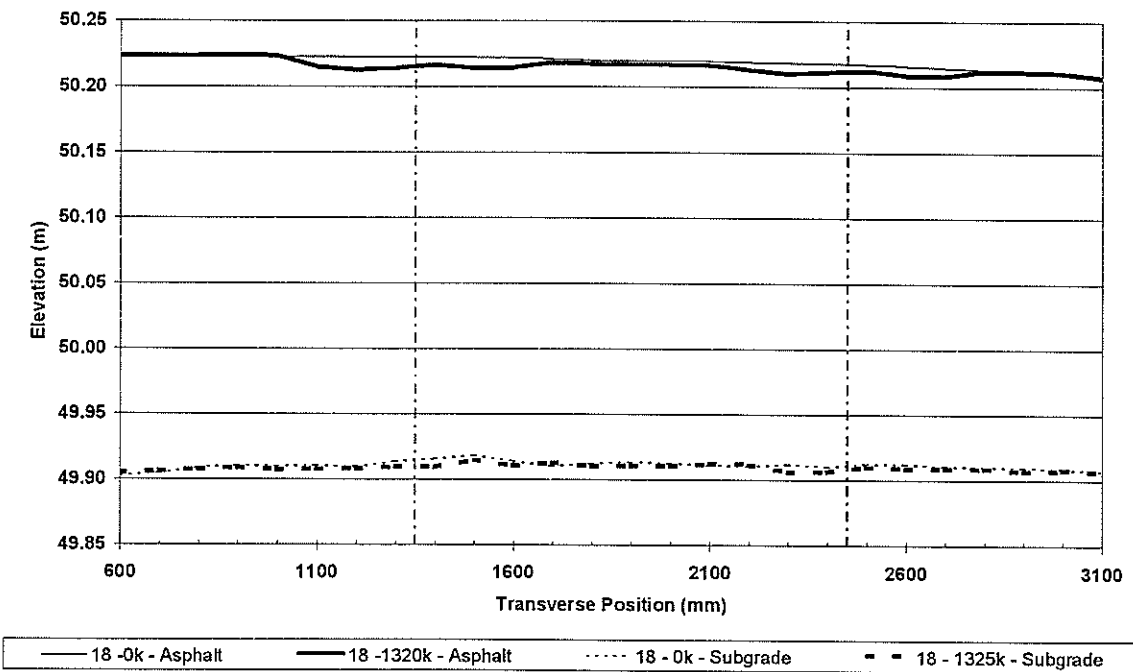


Figure A4 Section B post-mortem trench at station 18.

Appendix A

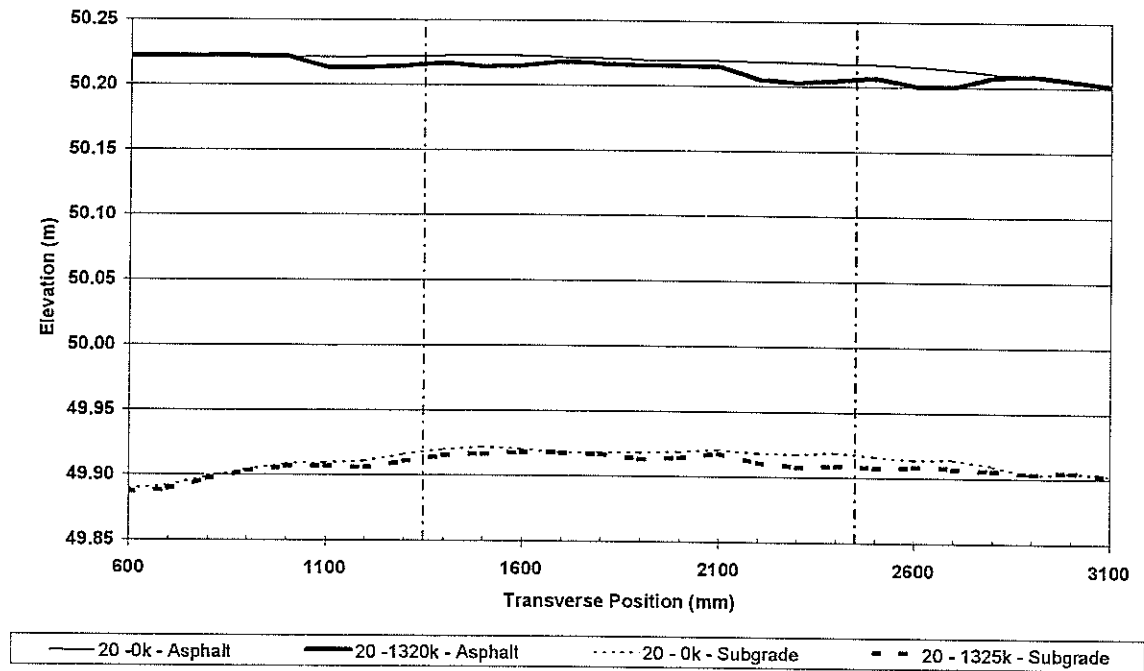


Figure A5 Section B post-mortem trench at station 20.

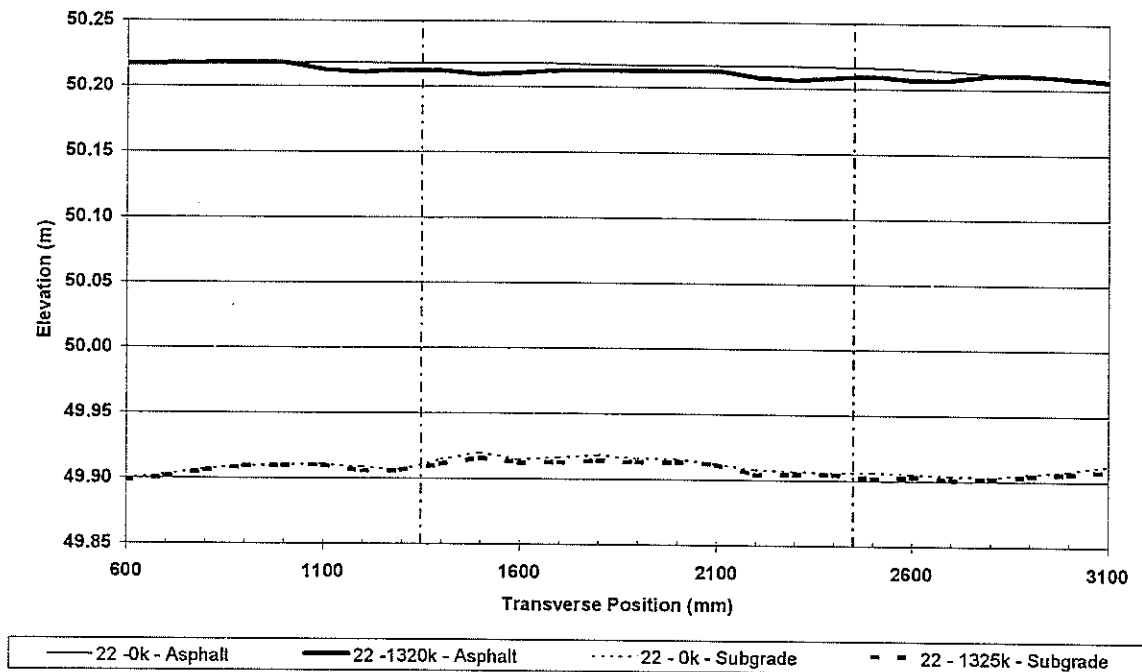


Figure A6 Section B post-mortem trench at station 22.

EFFECT ON PAVEMENT WEAR OF AN INCREASE IN MASS LIMITS

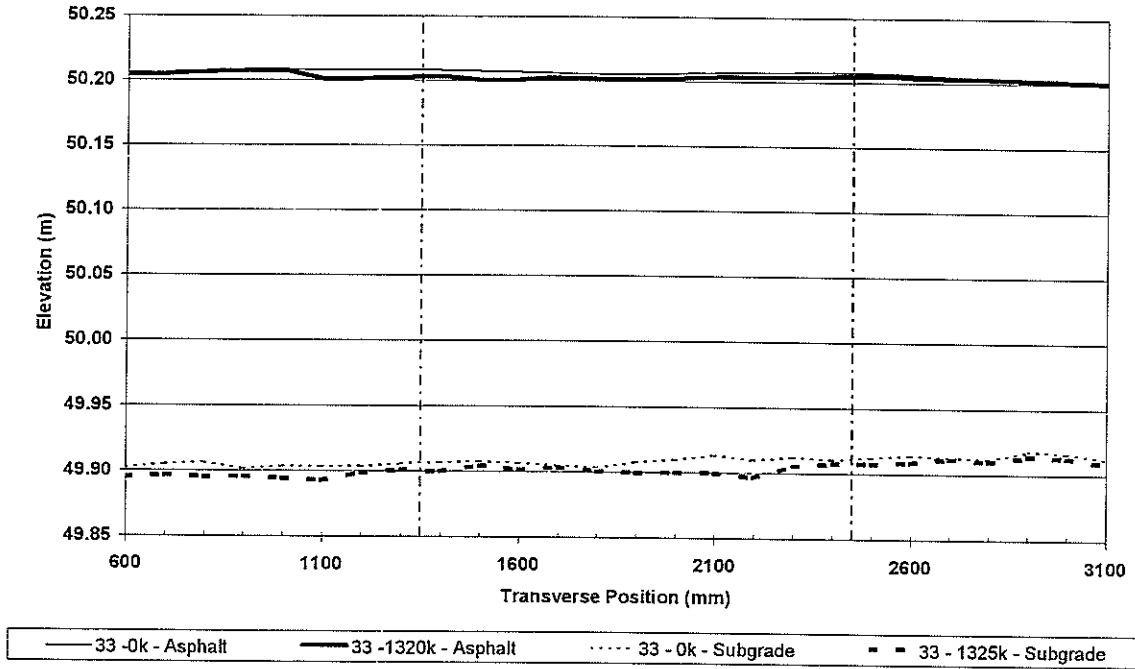


Figure A7 Section C post-mortem trench at station 33.

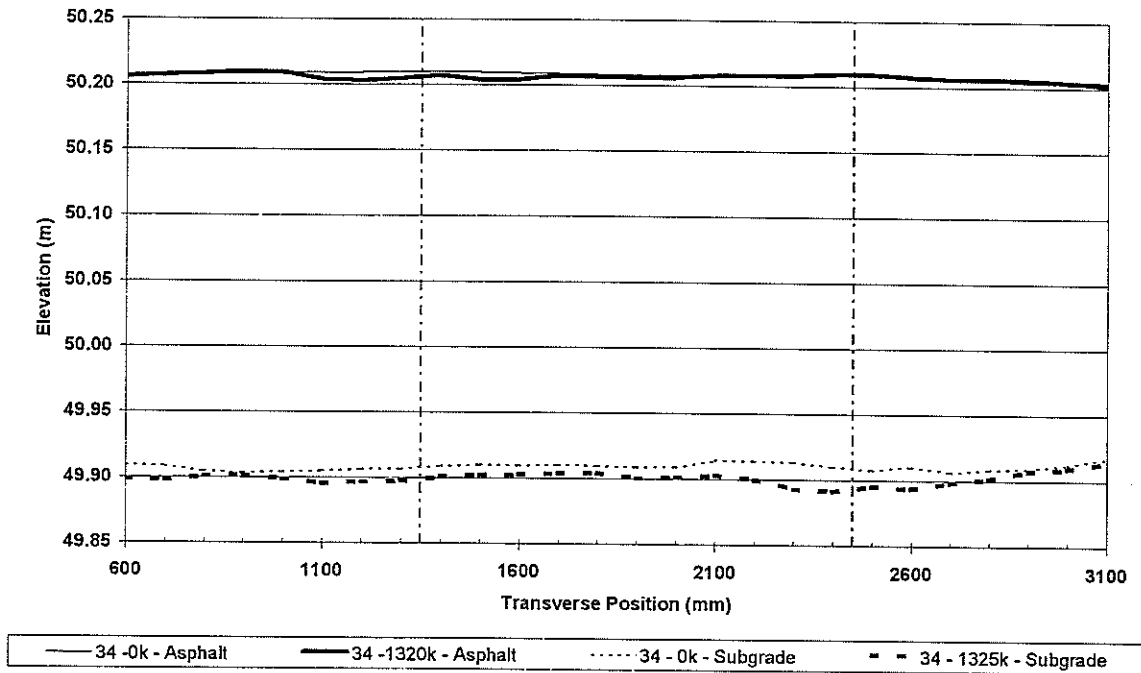


Figure A8 Section C post-mortem trench at station 34.



Appendix A

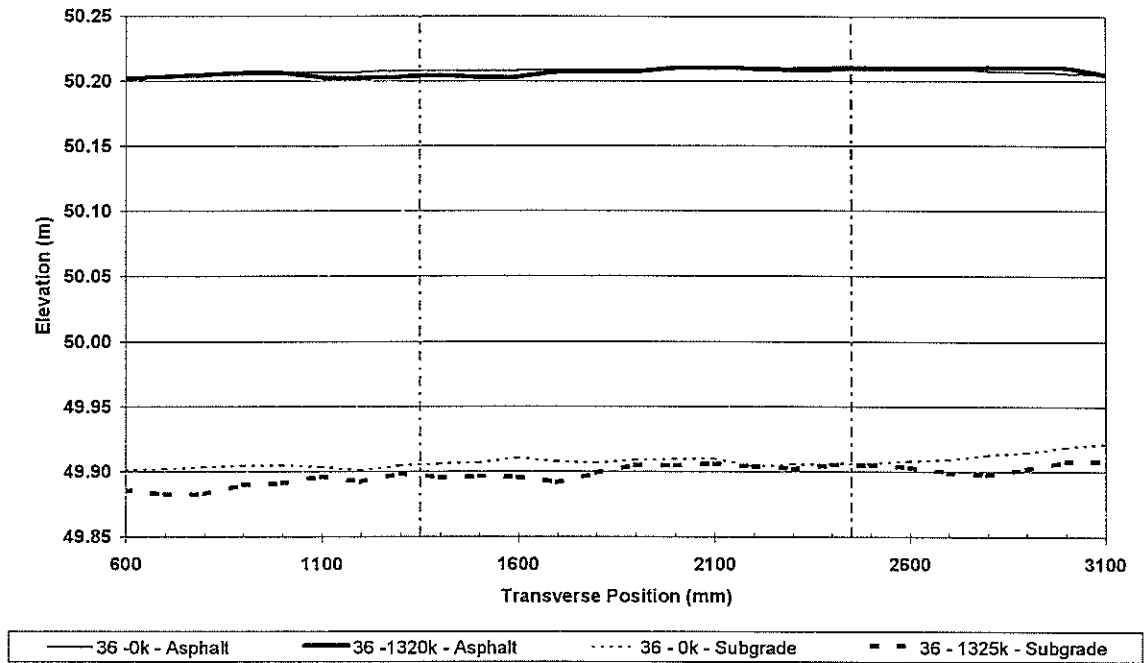


Figure A9 Section C post-mortem trench at station 36.

